Flood modelling of the Phetchaburi river basin

The importance of spatially distributed precipitation for flood modelling

K. Chen

TU Delft

Flood modelling of the Phetchaburi river basin

The importance of spatially distributed precipitation for flood modelling

by

K. Chen

to obtain the degree of Master of Science
at the Delft University of Technology,
to be defended publicly on June 25, 2025.

Thesis committee:	Prof. Dr. T.A. Bogaard,	TU Delft
	Dr. ir. O.A.C. Hoes,	TU Delft
	Assoc. Prof. P.P. Mapiam,	Kasetsart University

Preface

With this thesis, I am concluding my studies of the Environmental Engineering Master at the TU Delft. First, I would like to thank Thom, for guiding me through this project with your knowledge and for always being understanding. Every time I was not fully satisfied with my results or when I felt like it was not going as well as I had hoped, you would tell me that you were happy with the work I did. Your encouragement and belief in me made me believe in myself. I would also like to thank Olivier, for sharing your knowledge and insightful thoughts. I learned a lot of things I would otherwise not have thought of.

I would like to thank Punpim, for your valuable knowledge and for welcoming me in Thailand. I had an incredible time in Thailand working on this project and this would not have been possible without you. I would like to thank Tangkwa, for being a joy to work with. From providing me data I needed for this project to helping me with the arrangements for my stay in Thailand, you helped me a lot and I really appreciate it. I had a lot of fun learning about Thai culture and going sightseeing with you. And also thank you Poom, France, Ko and all the other students and researchers I met during my time in Thailand, I enjoyed working with you, learning from you, and having lunch with you all at Kasetsart University.

Thank you to all my fellow students, from the friends I made since the beginning of this Master to everyone I laughed with in the afstudeerhok these past months, you made my time here as a student unforgettable. It was wonderful to be surrounded by people who are motivated to make a positive change in the world.

Finally, I would like to thank my family and friends, for all your support and for believing in me. Thank you for being there for me when I needed it most. Thank you my dearest grandma, I will always remember you fondly. Thank you my dearest grandpa, you will always be here in my heart. This was all possible because you were there since the very beginning, taking little me to school on your bike everyday.

K. Chen
Delft, June 2025

Abstract

As flood intensities are increasing, Flood Early Warning Systems (FEWS) are becoming more crucial so the right mitigation measures can be taken. This study focused on the Phetchaburi river basin in Thailand, which experiences floods yearly. Currently, precipitation data from rain gauges are used in the FEWS for this region. However, weather radar is also available in Thailand. Weather radar is usually able to capture the spatial variability of precipitation in more detail. Therefore, this study aimed to research the effect of spatially distributed precipitation on flood modelling in the Phetchaburi river basin.

Using HEC-RAS, a hydrodynamic rainfall-runoff model of the Phetchaburi river basin was made. The area of interest was the middle reach of the Phetchaburi river and its two tributaries, lying in-between three reservoir dams upstream and the Phet Diversion Dam downstream. The Phetchaburi river and its tributaries were calibrated using measured dam outflow and water level data. Three types of precipitation data were used as input, namely homogeneous precipitation data and spatially distributed precipitation data obtained from weather radar and from rain gauges.

High infiltration rates were found for the Phetchaburi river basin. When homogeneous precipitation data was used as input, precipitation intensity would be too low, allowing all precipitation to infiltrate into the subsurface. Using homogenous precipitation data as input results in a underestimation of floods. On the contrary, precipitation intensities in spatially distributed precipitation data were high enough to exceed the soil infiltration capacity, leading to surface runoff and floods. When solely looking at the water balance, using precipitation data from weather radar and rain gauges as input lead to similar results. However, when it came to the water levels at specific locations, precipitation data from weather radar performed better. The density of the rain gauge network in the Phetchaburi river basin is too low to capture the spatial variability of the precipitation events in detail. This resulted in floods or the lack thereof at the wrong locations. Weather radar captures the spatial variability of precipitation in greater detail than rain gauges can. This study showed that using precipitation data from weather radar as input results in more accurate flood modelling in the Phetchaburi river basin.

Contents

List of Figures

List of Tables

Acronyms

DEM	Digital Elevation Model
FEWS	Flood Early Warning System
HEC-RAS	Hydrologic Engineering Centre-River Analysis System
RMSE	Root Mean Squared Error

1

Introduction

1.1. Background

Climate change has been a hot topic for years now, and not without reason. Global warming not only leads to an increase in drought intensity and duration, it also leads to higher intensity precipitation (Trenberth, 2011). This higher intensity precipitation will lead to higher runoff and therefore also higher intensity floods (Asadieh and Krakauer, 2017). Especially the Asia-Pacific region has suffered the most amount of natural disasters in the past few decades, with earthquakes, storms and floods being the ones with the most fatalities in this region (ESCAP, 2017). Among three different types of floods (coastal, flash and riverine), riverine floods are the most common type of floods in Asia and the Pacific (Kimuli et al., 2021).

With an increase in flood intensities, it becomes much harder to find realistic solutions to completely prevent floods. However, by implementing a Flood Early Warning System (FEWS), mitigation measures can be taken to reduce the amount of damages and people affected. A study by Kimuli et al. (2021) conducted a trend analysis for the Asia-Pacific region for the years 1990-2018 and found that while there is an upwards trend for the amount of flood occurrences, the trend of fatalities is declining. This could be a result of implementations of surveillance systems that help in forecasting and early warning so people can be evacuated on time and thereby reducing the amount of fatalities.

In this study, the focus will be on the Phetchaburi river basin in Thailand. This region experiences floods yearly. The river reach of interest for this study lies in between the Kaeng Krachan Dam upstream and the Phet Diversion Dam downstream. Aside from the main river, there are also two tributaries, each also originating from a reservoir. The three upstream reservoir dam outflows are directly impacting how much discharge flows through the rivers and the Phet Diversion Dam outflow decides how much water can leave the system. When the Phet Diversion Dam is closed during heavy precipitation events, the area right upstream of the diversion dam experiences floods. The water level can be higher than normal which typically only lasts a few days. However, opening the diversion dam can in turn also result in flooding of the area downstream of the dam. If it is known in time how a flood will propagate, the dam can be managed more efficiently. This way the flood upstream of the Phet Diversion Dam can be managed without causing significant problems downstream of the dam.

For this to work, implementing a FEWS that can accurately predict floods is crucial. Since heavy precipitation events can lead to floods, the accuracy of precipitation data is of great importance. Precipitation data from automatic rain gauge stations are readily available in Thailand. However, the amount of rain gauges in the study area is limited. Precipitation is a highly heterogeneous process on varying scales in space and time (Marani, 2005). If a network of rain gauges is not dense enough, the rain gauges will not be able to capture the spatial variability of a precipitation event in great detail since they are only point measurements (van de Beek et al., 2010). This might lead to inaccuracies when these point data are interpolated (Bárdossy and Pegram, 2013). The higher the intensity of a precipitation event, the higher the uncertainties are since precipitation tends to be more localized if the intensities are higher (Terink et al., 2018). Even in quite large basins (areas up to several thousand square kilometres), a dense network of rain gauges is mostly useful for estimating the total volume of a precipitation event in an area rather than for the characterization of its spatial variability (Nicótina et al., 2008).

Aside from rain gauges, weather radar is also available in Thailand, covering much larger areas. Precipitation data from weather radar are not being used in the FEWS yet. Radar is capable of capturing spatial and temporal information of precipitation in greater detail than a rain gauge network (van de Beek et al., 2010). A study by Terink et al. (2018) found that for a small rural lowland catchment at least 12 rain gauges per km^2 are needed to be able to capture the spatial variation in precipitation that is present in radar precipitation estimates. However, there are multiple errors that can be present in radar data, so corrections are needed to improve the quality of radar data (Uijlenhoet and Berne, 2008; Hazenberg et al., 2011). The goal of this study is therefore to assess the advantages and disadvantages of using precipitation data from weather radar as input for flood modelling in the Phetchaburi river basin.

1.2. Research question

The research question is as follows:

What is the effect of spatially distributed precipitation on the flooding of the middle reach of the Phetchaburi river?

Spatial and temporal variability in precipitation and river basin characteristics highly influence the stream flow (Singh, 1997). Multiple studies have studied the effect of spatially distributed precipitation on runoff modelling in comparison to non-spatially distributed precipitation (Arnaud et al., 2002; Gires et al., 2012) or compared different types of spatially distributed precipitation products (van de Beek et al., 2010; Silva et al., 2022). Since every region has its own unique physiographic and precipitation characteristics and different types of data available, it is interesting to see what the results for specifically the Phetchaburi region is.

1.3. Flood modelling

To answer the research question, a hydrodynamic rainfall-runoff model was made using the Hydrologic Engineering Centre-River Analysis System (HEC-RAS). This is a well known and widely used software for flood modelling. A 1D model is not capable of having precipitation as input. To be able to take the spatially distributed precipitation into account, it was decided to use a combined 1D-2D model. A study by Vozinaki et al. (2017) found that their combined 1D-2D model performed better than the 1D model if the DEM is of sufficiently high resolution.

1.4. Thesis outline

In Chapter 2 the study area and available data for this study are described. The methodology of the modelling of the study area is described in Chapter 3. In Chapter 4 the approach for the model runs in the study area is described. The results of the model runs are presented in Chapter 5. In Chapter 6 the model set up and results are discussed. Chapter 7 contains the conclusion of the study and recommendations for further studies.

2

Study area and available data

2.1. Study area

The Phetchaburi river basin is located in Thailand and covers most of the Phetchaburi province and partially the Samut Songkhram province and Ratchaburi province. It covers a total area of 6255 km^2. The wet season is from May to October, with an average annual precipitation of around 1110 mm in this basin. The annual minimum temperature is 27.9 °C and annual maximum temperature is 33.5 °C (Onarun et al., 2023).

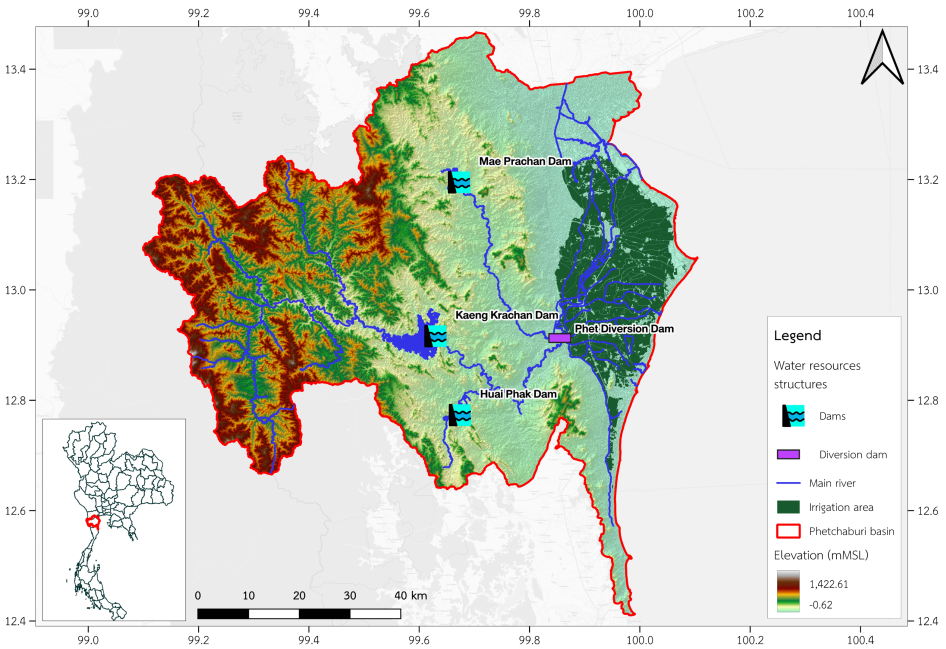

Figure 2.1: Topography map of the Phetchaburi river basin (Sreesomjai, 2024).

The river basin can be divided into three main regions. The most upstream reach of the Phetchaburi river is from the river source to the Kaeng Krachan reservoir. This upper region of the river basin is located in the Kaeng Krachan National Park. The most downstream reach of the Phetchaburi river is from the Phet Diversion Dam to the estuary. In this lower region of the river basin the Phetchaburi river branches out a lot. The main area of interest for this study is the middle region of the Phetchaburi river basin, with three rivers in between reservoir dams upstream and the Phet Diversion Dam downstream (Figure 2.1):

- The Phetchaburi river, the main river. Flows downstream of the Kaeng Krachan Dam to the Phet Diversion Dam. It is around 60 km long and has a slope of around 0.00067.
- The Mae Prachan river, a tributary of the Phetchaburi river. Flows downstream of the Mae Prachan Dam and joins the Phetchaburi river right before the Phet Diversion Dam. It is around 60 km long and has a slope of around 0.001.
- The Huai Phak river, a tributary of the Phetchaburi river. Flows downstream of the Huai Phak Dam and joins the Phetchaburi river halfway. It is around 14 km long and has a slope of around 0.002.

All three dams upstream are outlets of reservoirs. The Kaeng Krachan Dam also has a hydro-power generator. The reservoir behind the Kaeng Krachan Dam is a lake and is part of the Kaeng Krachan National Park. This park is a protected national park, covering the west half of the Phetchaburi province in mostly forest land (Figure 2.2). The east half of the province mostly consists of agricultural cropland. The study area is in the transition area between these two different types of land use so both types are present. When it comes to the soil, the study area consists of mostly acrisols and ambisols, with a bit of luvisols (Figure 2.3). In the study area, the geology mostly consists of graywacke and fluvial, alluvial and colluvial deposits (Appendix A).

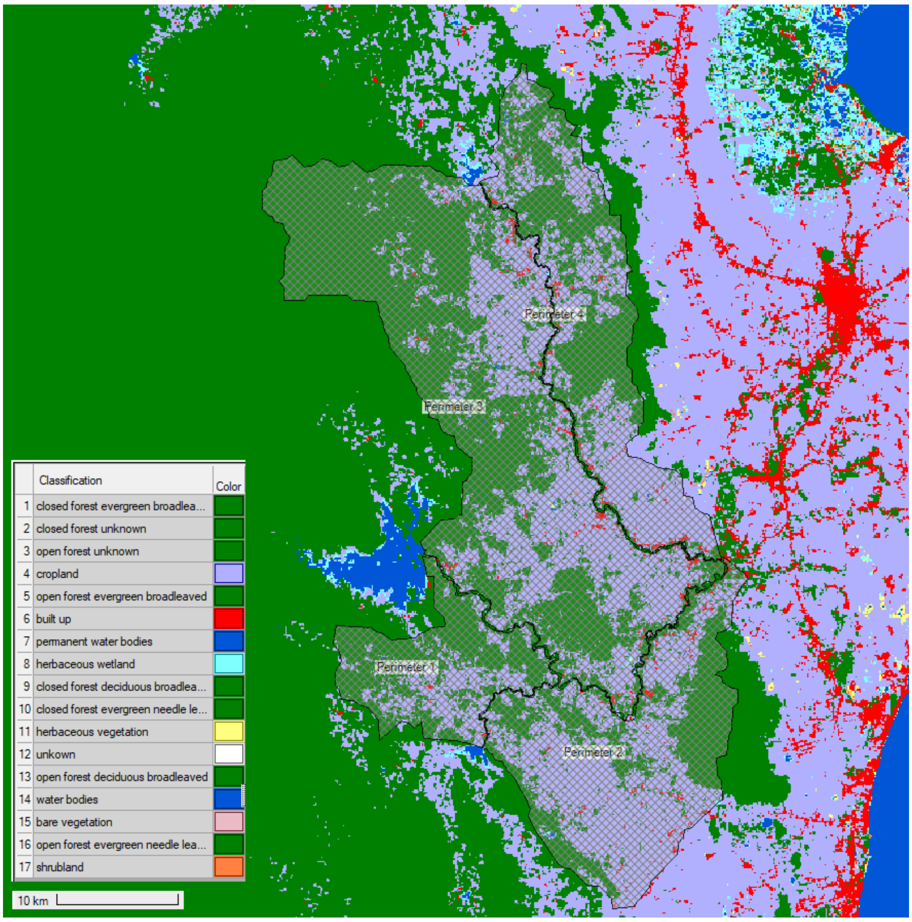

Figure 2.2: Land cover data of the Phetchaburi river basin obtained from Copernicus (Copernicus, n.d.). The study area is highlighted by the mesh.

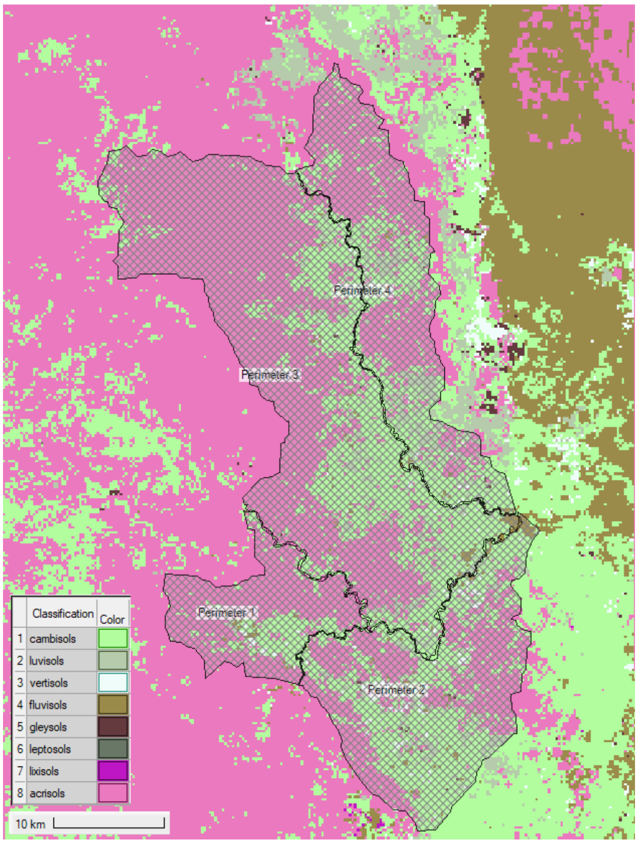

Figure 2.3: Soil data of the Phetchaburi river basin obtained from SoilGrids (SoilGrids, n.d.). The study area is highlighted by the mesh.

Just upstream of the Phet Diversion Dam, which is the outlet point of the study area, the Phetchaburi river floods every year. Flood walls of around two to three meters high have been built next to the river around three years before this study, however, these do not seem to significantly help. The rivers are filled with vegetation, especially downstream (Figure 2.4). However, there are plans to remove the vegetation from the river in the future.

Figure 2.4: Phetchaburi river around 1 km upstream of the Phet Diversion Dam.

2.2. Data

2.2.1. Digital Elevation Model

A Digital Elevation Model (DEM) of the area was used as basis for the 2D hydrological model. The one provided for this study has a resolution of 5 m, which is sufficient to capture the river basin in detail. However, since a DEM typically does not contain any information about the river bathymetry below the water surface, additional cross section data was needed. On top of that, the DEM is from 2003 and the river has changed and additional flood walls were built during this time, which also needed to be manually added in the model.

2.2.2. River bathymetry

Cross section data of the Phetchaburi river and the Mae Prachan river were provided for this study. No cross section data of the Huai Phak river were available. However, since the flow of this river is quite small and does not contribute much to the Phetchaburi river, it was decided to use the river bathymetry obtained from the DEM. Analysing all the cross section data, it became apparent that the depths in the DEM were not deep enough. This was mainly the case the more downstream the river we go. The amount of cross sections was not enough to directly put them into the model so it was decided to first draw the cross sections by hand. These initial cross sections were cut from the DEM and were manually changed to resemble the data. On top of that, the cross sections did not cover the downstream part of the Phetchaburi river. Additional cross sections were obtained through field work. Where possible, an Acoustic Doppler Current Profiler (ADCP) was used. At locations where this was not possible, a weighted measuring tape was used. These additional cross sections were also not directly put in the model but were used as a guideline to get a better approximation of the river bathymetry.

2.2.3. Dam outflow

As mentioned before, there are three reservoir dams upstream and one diversion dam downstream in the study area. The hourly operations worksheet of the Kaeng Krachan Dam, which releases into the Phetchaburi river, was obtained from the Electricity Generating Authority of Thailand (EGAT) for the years 2018-2023 (Figure 2.5). The total outflow of the Kaeng Krachan Dam consists of the outflow of the hydro-power generator, the irrigation outlet and the spillway. The hydro-power generator and irrigation outlet can discharge a maximum flow of 100 m^3/s. The spillway can discharge a maximum flow of 1380 m^3/s. The Kaeng Krachan Dam opens every morning to release water for recreational purposes and closes again every evening. Under normal circumstances, the discharge during the day is usually around 30 to 40 m^3/s and goes to zero during the night. There have been events where the outflow was much higher, reaching up to more than 350 m^3/s.

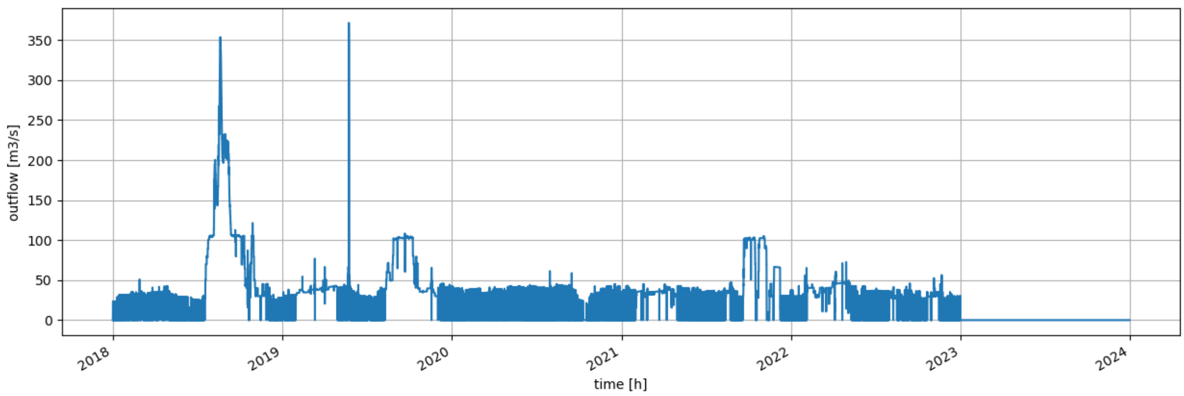

Figure 2.5: Hourly outflow data of the Kaeng Krachan Dam for the years 2018-2023.

For the Mae Prachan Dam and the Huai Phak Dam, only a daily hourly operations worksheet from the Royal Irrigation Department (RID) was available, for the years 2020-2023 (Figures 2.6 and 2.7). For both these reservoir dams, the total outflow consists of the outflow of the river outlet and the spillway. The outflow of the irrigation outlet goes directly to the irrigation channels and does not contribute to the outflow into the rivers. Under normal circumstances, the discharges of both these dams are low. However during the latter half of a year, higher discharges can also be observed with peaks up to 60 m^3/s.

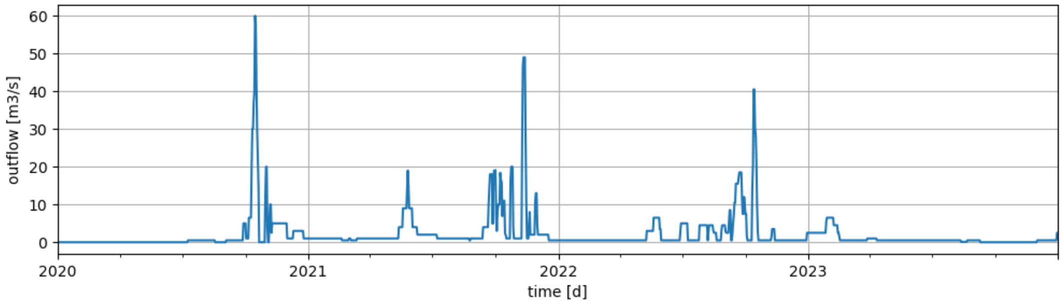

Figure 2.6: Daily outflow data of the Mae Prachan Dam for the years 2020-2023.

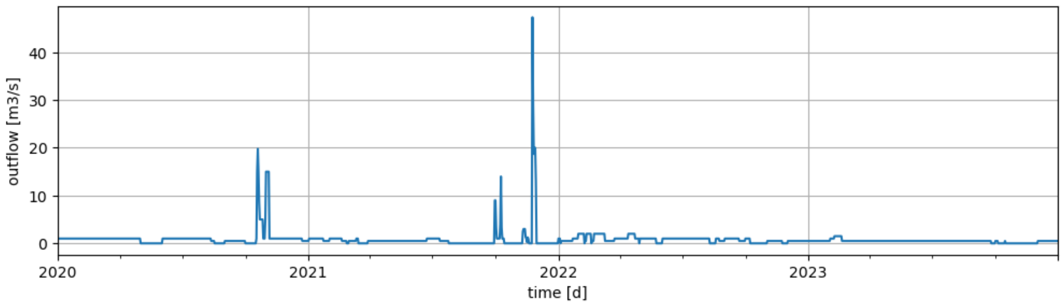

Figure 2.7: Daily outflow data of the Huai Phak Dam for the years 2020-2023.

For the Phet Diversion Dam, outflow and water level data of every 12 hours was available for the years 2019-2023 (Figure 2.8). The peaks in these data occur at the same time periods as the peaks in the reservoir outflows.

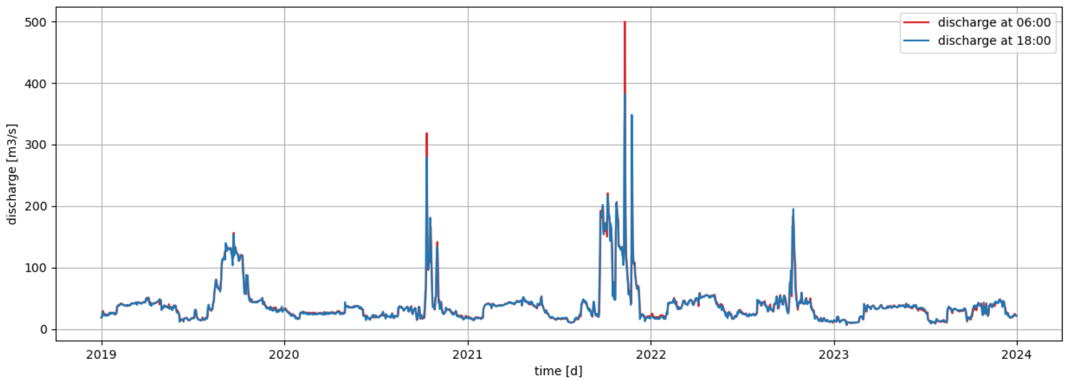

Figure 2.8: Outflow data of the Phet Diversion Dam for the years 2019-2023. The outflow is measured twice a day, with in red the outflow measured at 06:00 and in blue the outflow measured at 18:00.

2.2.4. Discharge and water levels in the rivers

Hourly discharge and water level data from several telemetering stations from the RID were provided for this study (Figure 2.9). The Phetchaburi river has three stations upstream of the Diversion Dam. Stations B.8A and B.9 have data from 2018 up to 2024, while station B.18 only has data from 2022 up to 2024 so it was decided to only use the first two stations. The Mae Prachan river has two stations, B.11 and B.6A, both have data from 2018 up to 2024. The Huai Phak river only has one station, B.8A, which has data from 2021 up to 2024. When comparing the water levels in the rivers (Figures 2.10 to 2.12) with the respective outflows of each river (Figures 2.5 to 2.7), the same peaks can be observed.

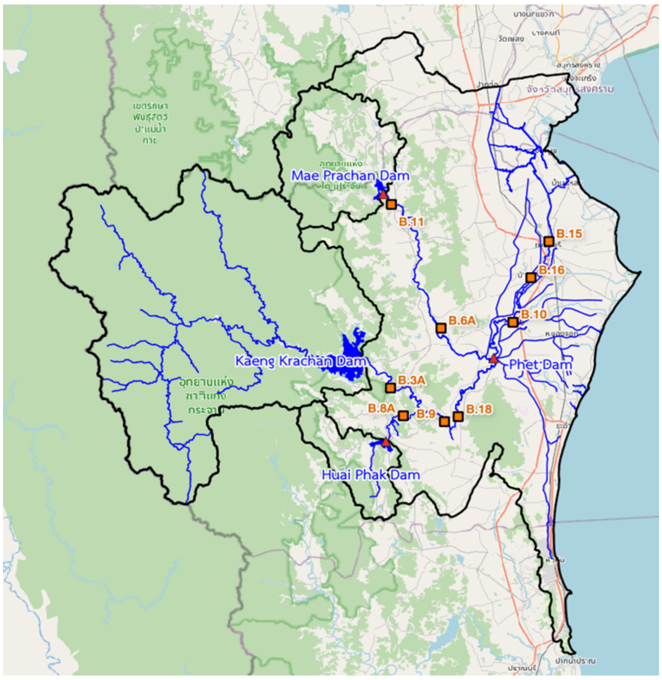

Figure 2.9: Locations of the telemetering stations (in orange) measuring discharge and water level in the Phetchaburi river, Mae Prachan river and Huai Phak river (Sreesomjai, 2024).

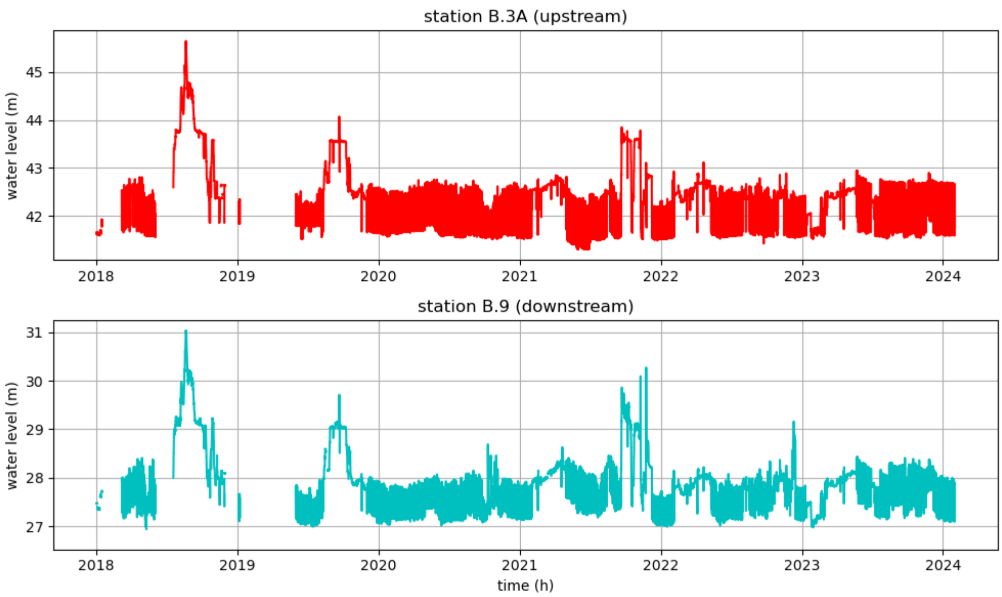

Figure 2.10: Hourly water levels measured at stations B.3A and B.9 in the Phetchaburi river for the years 2018-2024.

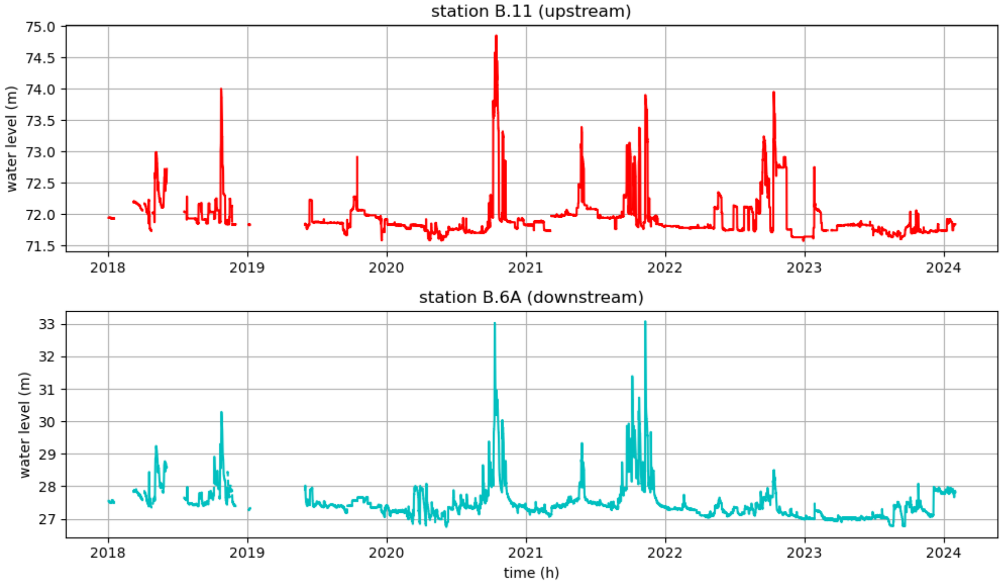

Figure 2.11: Hourly water levels measured at stations B.11 and B.6A in the Mae Prachan river for the years 2018-2024.

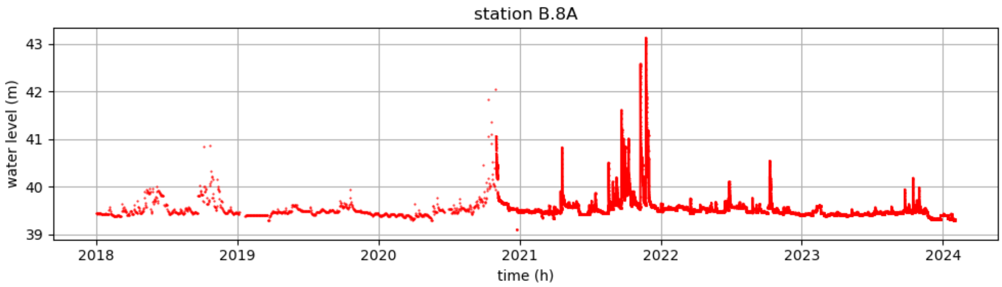

Figure 2.12: Hourly water levels measured at station B.8A in the Huai Phak river for the years 2018-2024.

2.2.5. Precipitation

Two types of measured precipitation data were available for this study, namely precipitation data from automatic rain gauge stations and precipitation data from a weather radar station. Precipitation data from the automatic rain gauge stations were obtained from the Hydro Informatics Institute (HII) and the Early Warning System (EWS) project of the Department of Water Resources in Thailand. In total there are 13 stations in the study area (Figure 2.13) with precipitation data available for the years 2018-2022 (Appendix B). These automatic rain gauges use a tipping bucket system for measuring precipitation. The automatic rain gauge stations from the HII have a temporal resolution of 15 minutes and the the ones from the EWS have a temporal resolution of 10 minutes. Precipitation data from both sources were resampled to hourly precipitation data for this study. The following rain gauge stations had issues or only had precipitation data for a limited time period:

- Station STN0281 registered some impossibly high values in 2020 and 2021 and did not register much precipitation in 2022.
- Stations BCAP, SWR007 and BPGD did not register any high peaks in 2021 during the wet season.
- Stations GALU and RMPT stopped working in 2021.
- Stations STN1647, STN1646 and STN1641 only became active in 2021.

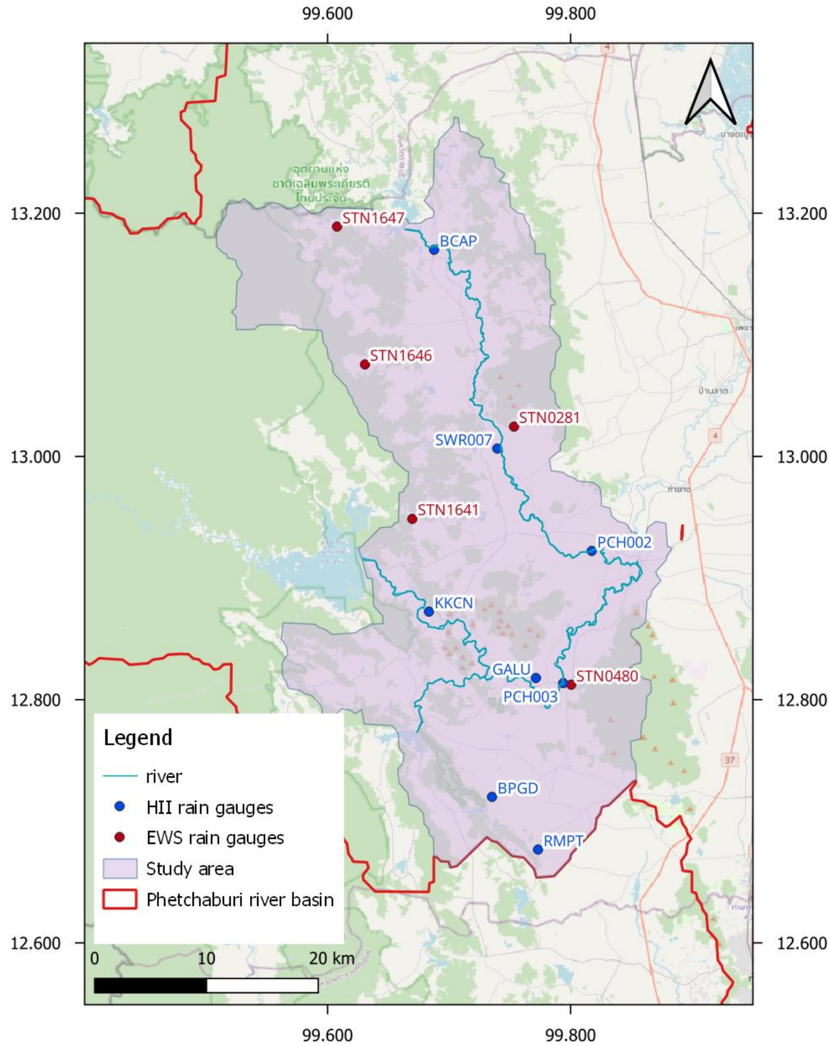

Figure 2.13: Locations of every automatic rain gauge station in the study area obtained from two Thai organisations.

Weather radar precipitation data products were obtained from the Department of Royal Rainmaking and Agricultural Aviation. The Sattahip radar station has a radius of 240 km and covers the entire study area. The station has a temporal resolution of 6 minutes. It is an S-band radar with a frequency of 2860 MHz and produces constant altitude plan position indicator (CAPPI) products at a level of 2.5 km. The provided weather radar precipitation data was corrected for this study. Precipitation data for the years 2018 and 2021 were available with time steps of an hour and grid sizes of 600 by 600 m.

3

Methodology of the modelling of the Phetchaburi river basin

3.1. Hydrodynamics background theory

1D unsteady flow

A 1D model can be run in HEC-RAS for either steady or unsteady flow. Steady flow is only applicable in situations where the flow is steady, gradually varied and one dimensional, and the river channels have small slopes. Since precipitation was included in this study and the 1D model was combined with the 2D model, unsteady flow needed to be used. Unsteady flow is computed based on conservation of mass (continuity) and conservation of momentum (HEC-RAS, 2024).

Conservation of mass states that the net rate of inflow into a control volume must be equal to the net rate of change of storage inside this volume. This is expressed with the continuity equation:

$$\frac{\partial A_T}{\partial t} + \frac{\partial Q}{\partial x} = q_t \tag{3.1}$$

where A_T is the total flow area, Q is the flow as a function of distance x and time t, and q_t is the lateral inflow per unit length.

Conservation of momentum states that the net rate of momentum entering a control volume plus the sum of all external forces acting on it must be equal to the rate of accumulation of momentum. This is expressed with the momentum equation:

$$\frac{\partial Q}{\partial t} + \frac{\partial QV}{\partial x} + gA(\frac{\partial z_s}{\partial x} + S_f) = 0 \tag{3.2}$$

where V is the control volume, g is the gravitational acceleration, A is the cross-sectional area, $\frac{\partial z_s}{\partial x}$ is the water surface slope, and S_f is the friction slope.

From these, Barkau (1982) derived a set of equations which is now the basis for the unsteady flow computation in HEC-RAS.

2D unsteady flow

In HEC-RAS, 2D unsteady flow can be computed using either the shallow water equations or the diffusion wave equations. In this study the diffusion wave equations were used for the computations.

The shallow water equations are derived from the Navier-Stokes equations. In the case that the horizontal length scale is much larger than the vertical length scale, conservation of mass implies that the vertical velocity is much smaller than the horizontal velocity. The Navier-Stokes vertical momentum equation then shows that the vertical pressure gradients are nearly hydrostatic. On top of that, if there are no baroclinic pressure gradients (variable density) and no strong wind forcing, it can be implied that the horizontal velocity is constant throughout the depth of the water. Vertical velocity and vertical derivative terms can then be neglected and the shallow water equations are obtained:

$$\frac{\partial u}{\partial t}+u\frac{\partial u}{\partial x}+v\frac{\partial u}{\partial y}-f_c v=-g\frac{\partial z_s}{\partial x}+\frac{1}{h}\frac{\partial}{\partial x}(\nu_{t,xx}h\frac{\partial u}{\partial x})+\frac{1}{h}\frac{\partial}{\partial y}(\nu_{t,yy}h\frac{\partial u}{\partial y})-\frac{\partial \tau_{b,x}}{\partial \rho R}+\frac{\partial \tau_{s,x}}{\partial \rho h}-\frac{1}{\rho}\frac{\partial p_a}{\partial x} \quad (3.3)$$

$$\frac{\partial v}{\partial t}+u\frac{\partial v}{\partial x}+v\frac{\partial v}{\partial y}-f_c v=-g\frac{\partial z_s}{\partial y}+\frac{1}{h}\frac{\partial}{\partial x}(\nu_{t,xx}h\frac{\partial v}{\partial x})+\frac{1}{h}\frac{\partial}{\partial y}(\nu_{t,yy}h\frac{\partial v}{\partial y})-\frac{\partial \tau_{b,y}}{\partial \rho R}+\frac{\partial \tau_{s,y}}{\partial \rho h}-\frac{1}{\rho}\frac{\partial p_a}{\partial y} \quad (3.4)$$

where

u, v: velocities in the Cartesian directions [L/T]

g: gravitational acceleration [L/T^2]

z_s: water surface elevation [L]

$\nu_{t,xx}, \nu_{t,yy}$: horizontal eddy viscosity coefficients in the x and y directions [L^2/T]

$\tau_{b,x}, \tau_{b,y}$: bottom shear stresses in the x and y directions [M/L/T^2]

R: hydraulic radius [L]

$\tau_{s,x}, \tau_{s,y}$: surface wind stresses in the x and y directions [M/L/T^2]

h: water depth [L]

f_c: Coriolis parameter [1/T]

p_a: atmospheric pressure [M/L/T^2]

The diffusion wave equations are an approximation of the shallow water equations. In shallow flow where the barotropic pressure gradient (gravity) term and the bottom friction terms are dominant in the momentum equations, the unsteady, advection, turbulence and Coriolis terms can be disregarded. After removing these terms and rearranging the equation, the final diffusion wave equation is obtained:

$$\frac{\partial h}{\partial t}=\nabla\cdot(\beta\nabla z_s)+S+q \quad (3.5)$$

where:

$$\beta=\frac{hR^{2/3}}{n}\left|\nabla z_s+\frac{1}{\rho g}\nabla p_a-\frac{\partial \tau_s}{\rho g h}\right|^{-1/2} \quad (3.6)$$

$$S=\nabla\cdot\left[\beta\left(\frac{1}{\rho g}\nabla p_a-\frac{\partial \tau_s}{\rho g h}\right)\right] \quad (3.7)$$

where ∇ is the gradient operator, ρ is the water density and τ_s is the wind shear stress.

3.2. Model structure

The Phetchaburi river basin was modelled using a combined 1D/2D model. The rivers were modelled in 1D and the floodplain was modelled in 2D (Figure 3.1). The boundaries of the system were the reservoir dams upstream and the Phet Diversion Dam downstream. The reservoirs themselves were not included in the model, only the outflows of the reservoir dams were used as boundary condition. Similarly for the Phet Diversion Dam, when water flows through the Phet Diversion Dam it leaves the system. This way the lower reach of the Phetchaburi river is excluded so there were no tidal influences on the study area.

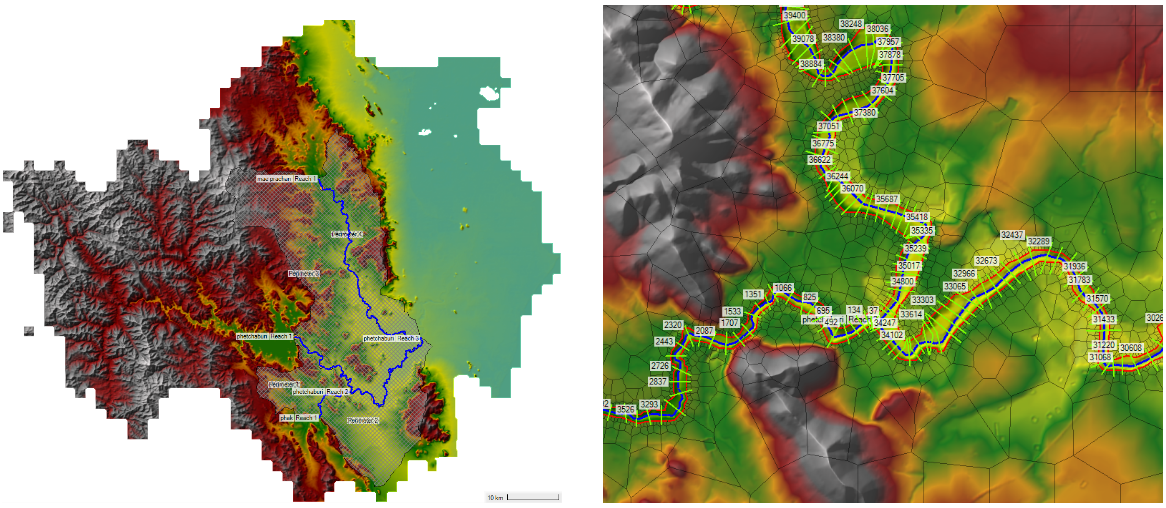

(a) Full extent of the DEM. The modelled study area is covered by the mesh.

(b) Close up of the model structure at the junction between the Phetchaburi river and the Huai Phak river, with the rivers in blue, riverbanks in red and cross sections in green.

Figure 3.1: Map and details of the model structure in HEC-RAS.

To model the rivers in 1D, three components were needed, namely the lines for the river, riverbanks and cross sections. These were manually drawn in. Cross section profiles were directly taken from the DEM, but as mentioned in Chapter 2, these cross sections were manually changed where necessary. On top of that, all three rivers also contain multiple weirs, which cause sudden large drops in depth at those locations. For simplicity these weirs were not in the model. However, large drops in depth caused computational instability, so to increase computational stability, the cross sections were modified to make the change in depths more gradual instead. In total there are 1332 cross sections with distances in the range of 50 to 200 m between each of them.

The base for the 2D component is the DEM with a resolution of 5 m. The rivers divide the terrain into four areas so four 2D flow areas with a computational mesh were needed, with in total 21890 cells. Since the conveyance of water is computed per cell, the resolution of the computational mesh decides how detailed this conveyance is modelled. The focus of this study was on how much and where the water enters the rivers, so the conveyance of water only needed to be more detailed close to the rivers. The cells adjacent to the riverbanks therefore have sizes of around 30 by 30 m and this increases up to 600 by 600 m the further away the cells are from the riverbanks. The DEM contains the full extent of the Phetchaburi river basin, however, only the study area is covered by the mesh and this is thus the extent of the model. The areas not covered by the mesh were excluded in the computations.

The 1D rivers and 2D flow areas are connected through lateral structures, which coincide with the riverbanks. As soon as the water level goes above the riverbanks, water leaves the 1D river and enters a 2D flow area. The flow of water can also go the other way, namely when precipitation falls on top of a 2D flow area and flows into the 1D river along the riverbanks.

3.3. Model parameters

Manning's roughness coefficient

The only parameter the Phetchaburi river and its tributaries were calibrated for was the Manning's roughness coefficient. The calibrations were done based on measured water level data from the telemetering stations. The Manning's roughness coefficient is an important parameter for computing the conveyance in a river and thus affects the wave celerity. The Manning's roughness coefficient varies along a river because of many factors like channel irregularities and vegetation for example (Watson, 1987; de Doncker et al., 2009). For simplicity, in this model the Manning's roughness coefficient was set to the same value everywhere along the river. The Manning's roughness coefficient can also vary across the river. Riverbanks usually contain more vegetation, resulting in higher Manning's roughness coefficients than in the main channel. The Manning's roughness coefficient can be set for the right riverbank, the left riverbank and the main channel. For simplicity, the left and right riverbanks were set to the same value with this value being higher than the value for the main channel. To determine the total conveyance in HEC-RAS, the river is first subdivided into multiple sections based on the different Manning's roughness coefficients. In each subdivision the conveyance is then calculated from the following Manning's equation (HEC-RAS, 2024):

$$Q = KS_f^{1/2} \tag{3.8}$$

$$K = \frac{1.486}{n} AR^{2/3} \tag{3.9}$$

where

K: conveyance for subdivision

n: Manning's roughness coefficient for subdivision

A: flow area for subdivision

R: hydraulic radius for subdivision (area / wetted perimeter)

S_f: slope of the energy gradeline

For the 2D floodplains, the Manning's roughness coefficients were based on the values by HEC-RAS (n.d.), which are adapted from Chow (1959), for each land use type.

Infiltration

When precipitation falls in the Phetchaburi river basin, part of it will infiltrate into the subsurface while the remaining part becomes surface runoff and contributes to the floods. HEC-RAS has three different methods to compute infiltration. For this study it was decided use the Deficit and Constant method (Figure 3.2). In this method the soil is a single homogeneous layer where the moisture is evenly distributed throughout the soil layer. During a precipitation event, precipitation infiltrates into the soil layer until the moisture deficit is satisfied. Once the maximum deficit is satisfied, the moisture leaves the system with a constant percolation rate. When the precipitation rate is higher than the percolation rate, the difference becomes excess precipitation, which enters the system (HEC-RAS, 2024). The amount of precipitation that infiltrates into the soil layer leaves the system and does not contribute to runoff. Groundwater flow is outside the boundaries of this study.

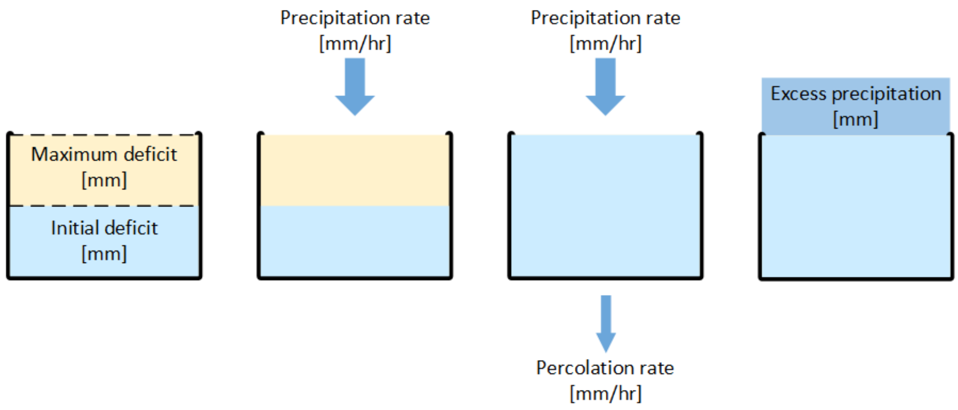

Figure 3.2: A visualisation of each step in the Deficit and Constant method. When the maximum deficit is satisfied, excess precipitation becomes surface runoff.

In between precipitation events water can also leave the system through evaporation. However, since this study was focused on single precipitation events, evaporation could be neglected. The only three parameters of interest were then: the maximum deficit [mm], the initial deficit [mm] and the potential percolation rate [mm/hr]. The infiltration layer was made using the land cover layer. For simplicity, the only spatial variation in the percolation rate was based on two types of land use. A higher percolation rate for forest land use types and a lower percolation rate for all other land use classes such as cropland and built up.

3.4. Boundary conditions

Dam outflow

The upstream boundary conditions of the rivers are the outflows of the three reservoir dams. The inputs are in the form of hourly flow hydrographs. These flow hydrographs cannot have zero flow because the model becomes numerically unstable if there is no flow. The minimum flow for which the model can run is 5 m^3/s for each river. The downstream boundary condition is the outflow of the Phet Diversion Dam. The input for this boundary condition can be in the form of a stage or flow hydrograph.

Precipitation

The last input is precipitation. As mentioned before, the amount of precipitation that is not lost to infiltration becomes excess precipitation which becomes runoff. For each cell on the computational mesh, the water surface elevation and the velocity and its direction are computed using the diffusion wave equations mentioned before (HEC-RAS, 2024). These parameters decide the conveyance of the runoff.

In HEC-RAS precipitation data can be in the form of gridded data, point data or a constant value. In this study, all three types of data were used and compared. The gridded data used in this study was in the form of weather radar precipitation data. These data were obtained from the weather radar station as mentioned in Chapter 2. These are spatially distributed precipitation data. Precipitation data from rain gauges is a form of point data and this is also a form of spatially distributed precipitation data. The decision to use the Thiessen Polygon method (Thiessen, 1911) was made to interpolate the point data. The rain gauge data was scaled when necessary, so that the total amounts of precipitation that falls in the study area are the same. In case of precipitation in the form of a constant value, precipitation falls on the whole computational mesh with a constant value. In this study this was used for homogeneous precipitation. Homogeneous precipitation is an artificial precipitation scenario where the total precipitation obtained from the weather radar station is evenly spread out over the duration of the precipitation event and homogeneously spread out over the whole area. This type of precipitation data is thus not spatially distributed. For all three types of precipitation the total amount of precipitation was the same, the only difference was how and whether they were spatially distributed.

3.5. Model schematisation

The final model schematisation can be seen in Figure 3.3. The blue boxes represent the two components of the model. The white boxes represent the input and output of the model. The arrows represent how the different components are connected and how the water flows.

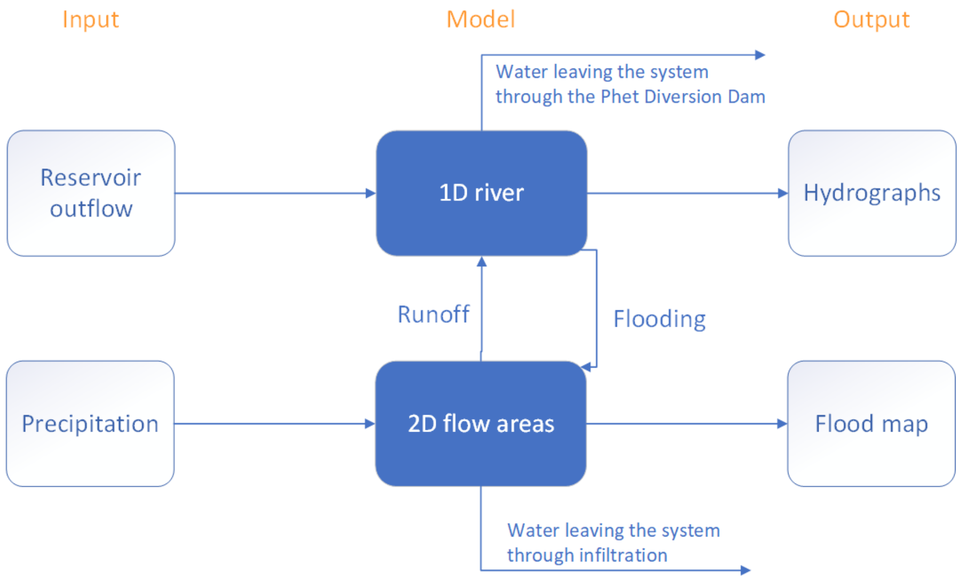

Figure 3.3: Schematic representation of the model components and boundaries.

Reservoir outflows directly enter the rivers and thus decide the discharge in the rivers. Precipitation falls on the flow areas, where part of the precipitation will leave the system through infiltration. The remaining precipitation becomes runoff and enters the rivers, contributing to the discharge in the rivers. Water leaves the Phetchaburi river through the Phet Diversion Dam. If it starts flooding on any of the rivers, water enters the flow areas. Two types of outputs are produced at the end of each model run, namely hydrographs, for water level and discharge, and a flood map.

4

Model runs approach for the Phetchaburi river basin

4.1. Calibration of the Phetchaburi river and its tributaries

An increase in water level upstream could contribute to a flood downstream. It is thus important that the velocity with which a wave propagates, which is called the wave celerity, is correct. The wave celerity depends on the Manning's roughness coefficient in a river. The Manning's roughness coefficients were not known for the Phetchaburi river and its tributaries so these had to be calibrated. Since hourly outflow data of the Kaeng Krachan Dam and hourly water level data of two telemetering stations in the Phetchaburi river was available, the wave celerity was known so the Phetchaburi river was thus calibrated on these data. The Kaeng Krachan Dams opens during the day and closes during the night under normal circumstances, making the oscillations in these data ideal for calibrating the Phetchaburi river on. However, for the Mae Prachan river and Huai Phak river this was not possible since the reservoir dam outflows for these rivers had a temporal resolution of a day so no oscillations were observed. The Manning's coefficients for these rivers were thus only calibrated based on water level. No precipitation was present during the calibration phase to make sure no other factors influenced the water levels.

4.2. River capacity

After calibrating the Phetchaburi river, the river capacity could be found. When no precipitation is present, only the outflows of the reservoir dams contribute to the discharge in the Phetchaburi river. It was therefore interesting to find out what the maximum amount of reservoir outflow could be before the Phetchaburi river started to flood. Since the discharge and water level downstream in the Phetchaburi river is decided by the outflow of the Phet Diversion Dam, the amount of discharge it takes before the river starts to flood partially depends on the outflow of the Phet Diversion Dam. To find the river capacity there were thus two scenarios, namely the "closed" scenario and the "open" scenario. The closed scenario represented a situation where the Phet Diversion Dam is closed and the outflow of the Phet Diversion Dam cannot increase. The open scenario represented a situation where the outflow of the Phet Diversion Dam changes with the discharge of the river, so the outflow of the Phet Diversion Dam could increase when the discharge increased.

4.3. Selecting and assessing infiltration parameters and precipitation data types

Scenarios

The focus of this study was on flood modelling during precipitation events. As explained in Chapter 3, part of the total amount of precipitation infiltrates into the subsurface and the excess precipitation becomes runoff. since the three types of precipitation data are differently spatially distributed, the result for each precipitation data type could be different for the same infiltration parameter. It was therefore decided to run different infiltration parameters simultaneously with different precipitation data types. Since the model was only run for single precipitation events, the maximum deficit and initial deficit did not play a big role so these were set to a constant value. Only the percolation rate was of interest in this study. The percolation rate decides how fast precipitation infiltrates into the subsurface. For the percolation rate, four scenarios were defined:

- No infiltration: this is to see what the situation would look like if infiltration is ignored in the river basin.
- Percolation rate of 3 mm/hr: a small percolation rate to see if this already has a big influence on the results.
- Percolation rate of 5 mm/hr: a slightly bigger percolation rate to see what the effect is of a small increase in the percolation rate.
- Percolation rate varying from 5 to 20 mm/hr: to take into account the different land cover types. A high percolation rate of 20 mm/hr for forest land and a low percolation rate of 5 mm/hr for all else.

These four infiltration scenarios were run in combination with homogeneous precipitation and spatially distributed precipitation data from the weather radar station and automatic rain gauge stations. In total there were thus twelve scenarios (Figure 4.1). These twelve scenarios were then run for two precipitation events.

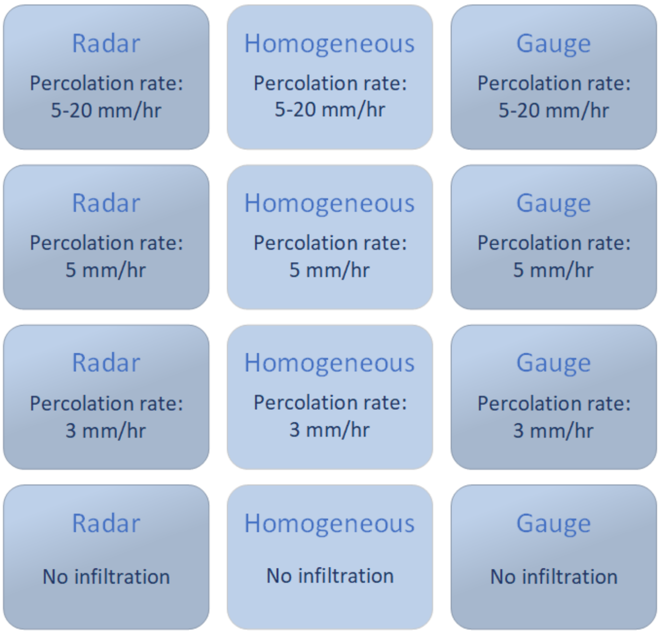

Figure 4.1: The infiltration and precipitation data type scenarios. Four infiltration scenarios are combined with three precipitation data types, resulting in a total twelve scenarios per precipitation event.

To evaluate the results, a water balance diagram was made for each scenario. From these the total inflows and outflows of the whole study area could be analysed. Using the water balance diagrams, the percentage of precipitation that did not infiltrate into the soil and thus became runoff was calculated. To analyse the water level in each river, hydrographs were plotted for each telemetering station in the Phetchaburi river and its tributaries. The hydrographs were visually corrected for a bias. After the bias correction, the root mean squared error (RMSE) for each hydrograph was calculated. The RMSE was calculated as follows:

$$RMSE = \sqrt{\frac{1}{n}\sum_{i=1}^{n}(y_i - \hat{y}_i)^2} \tag{4.1}$$

where n is the total amount of measurements, y is the measured value, and $\hat{y}$ is the modelled value.

Precipitation event selection

The Geo-Informatics and Space Technology Development Agency (GISTDA) is a Thai space agency and research organisation involved in remote sensing. GISTDA has a decision support system for disaster management that provides geospatial information on floods, forest fires and droughts. Flood maps of historical floods in Thailand can be found on their website. For the middle reach of the Phetchaburi river basin there was only one flood recorded in 2018 (Figure 4.2). However, the date of this flood is unknown. Upon inspecting the precipitation data for the year 2018, there did not seem to be any significant precipitation events compared to other years (Appendix B). However, upon inspecting the dam outflows (Figure 2.5) and the water levels measured by the telemetering stations (Figure 2.10), it is likely that the cause of the flood was the high outflow of the Kaeng Krachan Dam over a time period of several months. Therefore, the events were chosen based on high precipitation peaks instead.

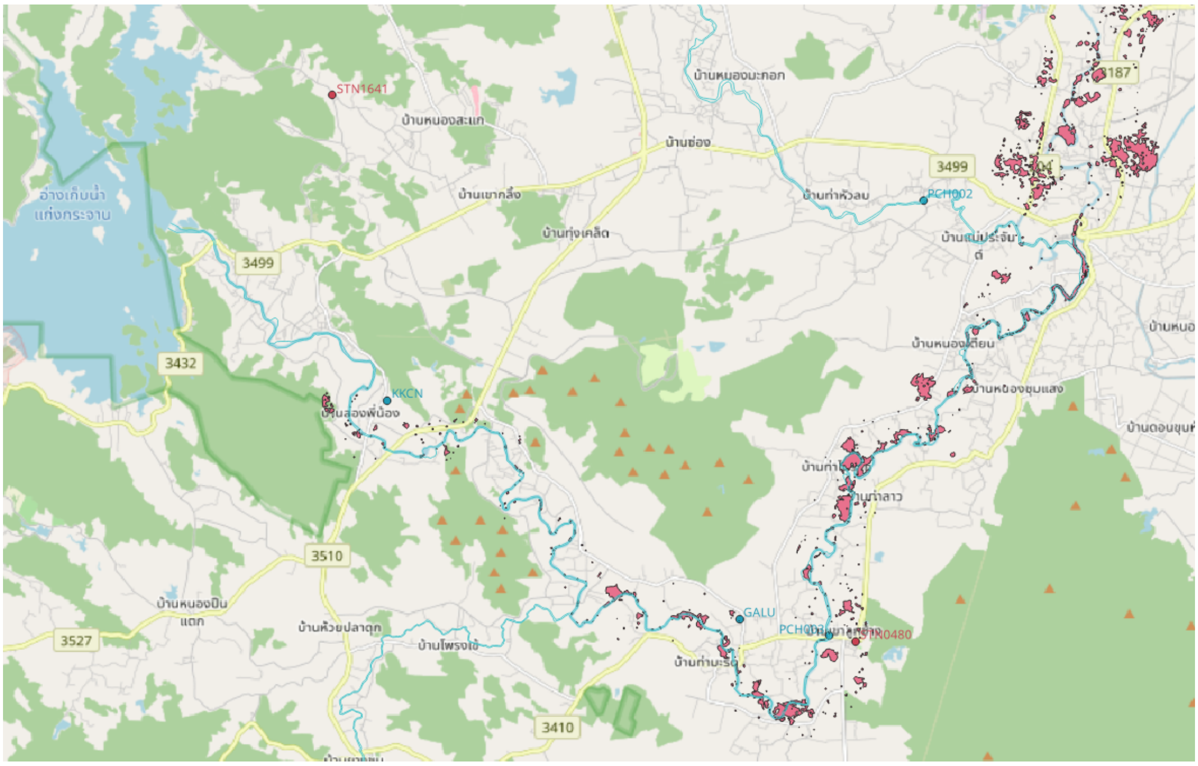

Figure 4.2: Flood map of a flood event at the Phetchaburi river in 2018, obtained from GISTDA.

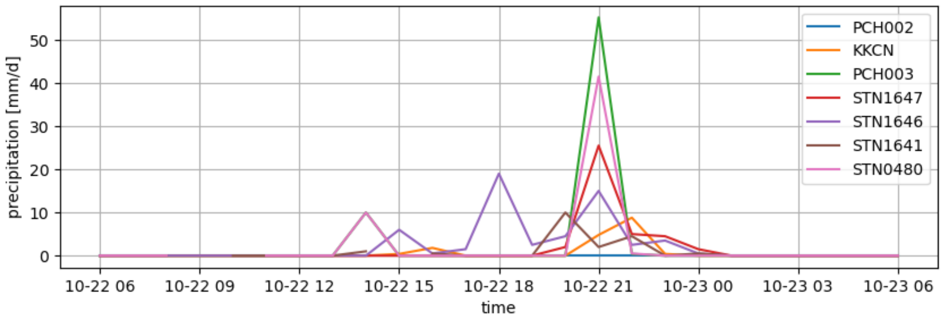

Figure 4.3: Hourly precipitation data in the study area for the time period 2021-10-22 06:00:00 to 2021-10-23 06:00:00.

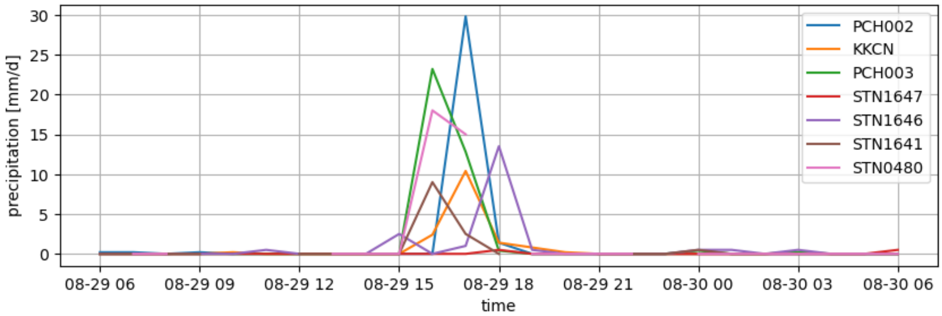

Figure 4.4: Hourly precipitation data in the study area for the time period 2021-10-22 06:00:00 to 2021-10-23 06:00:00.

After analysing the precipitation data from the automatic rain gauge stations, several precipitation events from the year 2021 were considered. After analysing the data of the weather radar station, two precipitation events were selected that had no missing data. The first precipitation event was from 2021-10-22 to 2021-10-23 (Figure 4.3) and the second precipitation event was from 2021-08-29 to 2021-08-30 (Figure 4.4). In total there were seven automatic rain gauge stations available for the year 2021.

5
Results

5.1. Calibration of the Phetchaburi river and its tributaries

The Manning's roughness coefficients for the rivers were calibrated based on two historical events. As mentioned in Chapter 2, under regular circumstances the Kaeng Krachan Dam opens during the day and closes during the night. The noticeable rising and lowering of the water level in the data was ideal for calibrating the Manning's roughness coefficient in the Phetchaburi river on wave celerity. Event 1.1 was a regular period from 2020-01-01 to 2020-01-05 (Figure 5.1a). Event 1.2 was from 2021-04-01 to 2021-04-05. This was a period where the Kaeng Krachan Dam did not fully close like it did during event 1.1, but oscillations in the dam outflow and water levels were still present (Figure 5.1b). For the Mae Prachan Dam and the Huai Phak Dam, the outflows are daily as mentioned before. This made it impossible to calibrate these rivers on any oscillations so these rivers were only calibrated based on water level. The Manning's roughness coefficient of the riverbanks of all the rivers were kept constant with a value of 0.06.

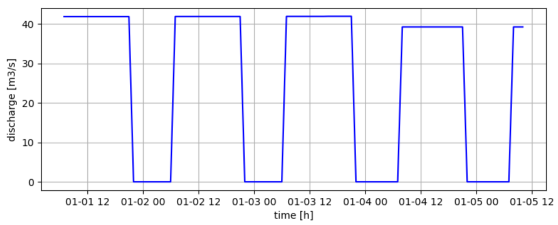

(a) Event 1.1 (2020-01-01 07:00:00 to 2020-01-05 10:00:00)

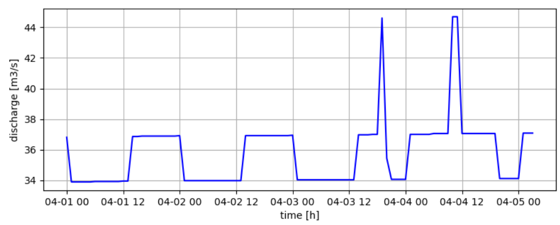

(b) Event 1.2 (2021-04-01 00:00:00 to 2021-04-05 03:00:00)

Figure 5.1: Hourly outflow data of the Kaeng Krachan Dam for the selected events.

Calibration of the Phetchaburi river

For event 1.1, the outflow of the Kaeng Krachan Dam was zero at night so an additional base flow of 10 m^3/s was added to replace the zero flow in the input flow hydrograph. The resulting modelled hydrographs of the water levels (Figure 5.2) match up with the measured water levels after a bias correction, with RMSE of smaller than 20 cm (Table 5.1). For event 1.2, no additional base flow was added. The modelled hydrographs for event 1.2 (Figure 5.3) also match up with the measured hydrographs after a bias correction, with RMSE of smaller than 3 cm (Table 5.1). The Manning's roughness coefficient in the Phetchaburi river was 0.03 for these results, which falls in the expected range of values.

Table 5.1: Bias and RMSE of the modelled water levels after calibrating the Phetchaburi river.

Station	Bias event 1.1 [m]	RMSE event 1.1 [m]	Bias event 1.2 [m]	RMSE event 1.2 [m]
B.3A (upstream)	-0.060	0.175	-0.327	0.011
B.9 (downstream)	0.136	0.187	-0.071	0.026

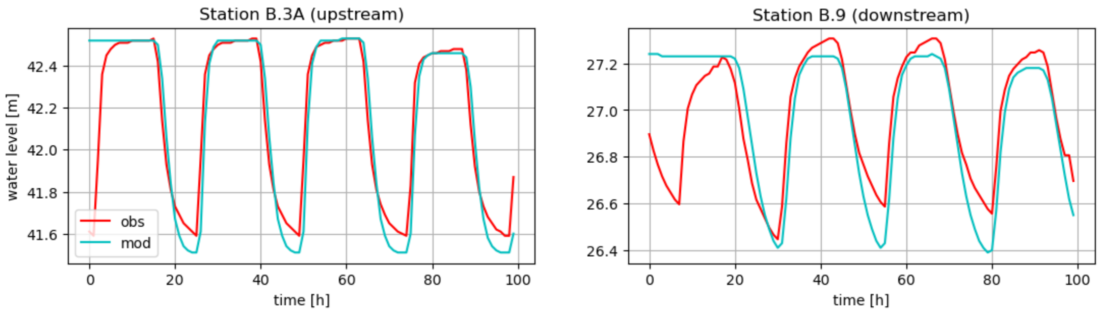

Figure 5.2: Hydrographs of the observed and modelled water levels in the Phetchaburi river for event 1.1.

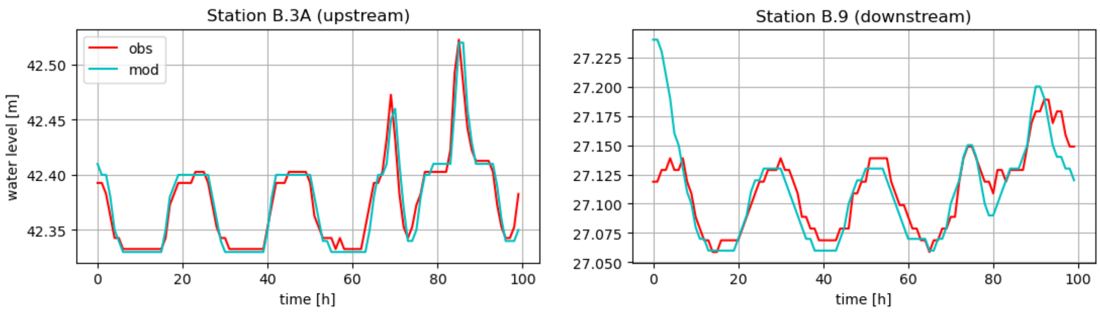

Figure 5.3: Hydrographs of the observed and modelled water levels in the Phetchaburi river for event 1.2.

Calibration of the Mae Prachan river

For event 1.1, the outflow of the Mae Prachan Dam was zero, however the measured water levels were not zero so a base flow of 15 m^3/s was used. The resulting modelled hydrographs (Figure 5.4) were corrected for a bias, resulting in RMSE of smaller than 4 cm (Table 5.2). For event 1.2, the outflow of the Mae Prachan Dam was only 1 m^3/s according to the measured data. Again a base flow of 15 m^3/s was used instead. The resulting modelled hydrographs (Figure 5.5) were corrected for a bias, resulting in RMSE of smaller than 2 cm (Table 5.2). For both events oscillations in the measured water levels can be observed. However, the amplitudes of these oscillations are small, which explains the small RMSE. The biases are a bit higher despite the fact that the Mae Prachan river was calibrated on water levels. This is explained by the fact that the modelled water levels for station B.11 were a bit too low while the modelled water levels for station B.6A were a bit too high, so these results are the optimal compromise. The Manning's roughness coefficient in the Mae Prachan river was 0.03 for these results.

Table 5.2: Bias and RMSE of the modelled water levels after calibrating the Mae Prachan river.

Station	Bias event 1.1 [m]	RMSE event 1.1 [m]	Bias event 1.2 [m]	RMSE event 1.2 [m]
B.11 (upstream)	-0.024	0.037	-0.127	0.008
B.6A (downstream)	0.129	0.024	0.134	0.021

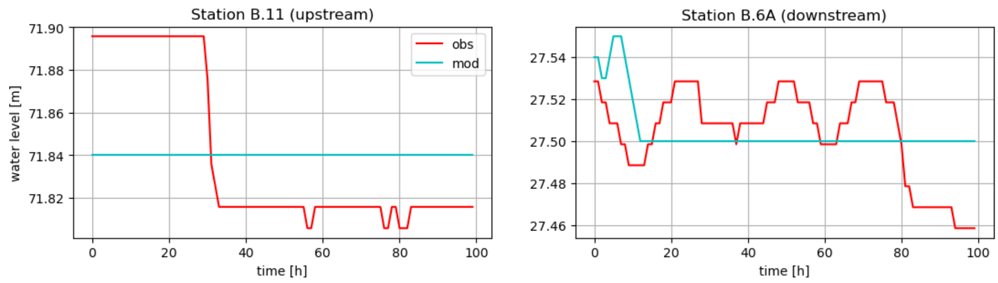

Figure 5.4: Hydrographs of the observed and modelled water levels n the Mae Prachan river for event 1.1.

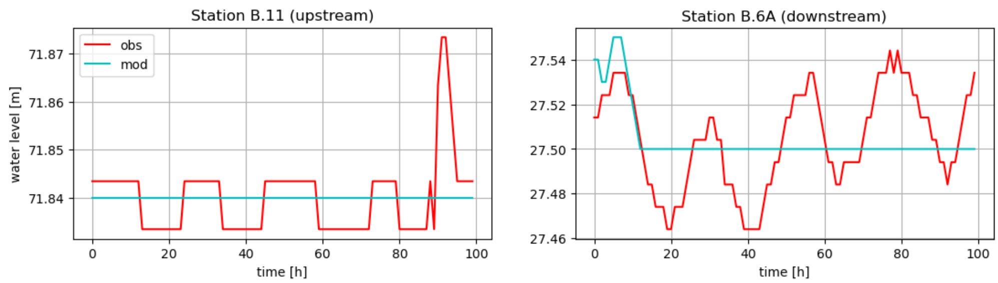

Figure 5.5: Hydrographs of the observed and modelled water levels in the Mae Prachan river for event 1.2.

Calibration of the Huai Phak river

For event 1.1, the outflow of the Huai Phak Dam was only 1 m^3/s in the measured data. It was thus decided to use an outflow of 5 m^3/s instead. Since no oscillations were present in the modelled or measured water levels, the modelled hydrograph (Figure 5.6) is the exact same as the measured hydrograph after a bias correction, with a RMSE of 0 m (Table 5.3). For event 1.2, the outflow of the dam was 0.5 m^3/s in the measured data. An outflow of 5 m^3/s was also used for this event. The modelled hydrograph (Figure 5.6) had a RMSE of smaller than 1 cm after a bias correction (Table 5.3). For both events, the modelled water levels are higher than the measured water levels. It was not possible to model lower water levels since neither the reservoir dam outflow nor the Manning's roughness coefficient could go lower because of computational instability. The Manning's roughness coefficient in the Huai Phak river was 0.035 for these results.

Table 5.3: Bias and RMSE of the modelled water levels after calibrating the Huai Phak river for event 1.1 and event 1.2.

Station	Bias event 1.1 [m]	RMSE event 1.1 [m]	Bias event 1.2 [m]	RMSE event 1.2 [m]
B.8A	0.260	0	0.193	0.007

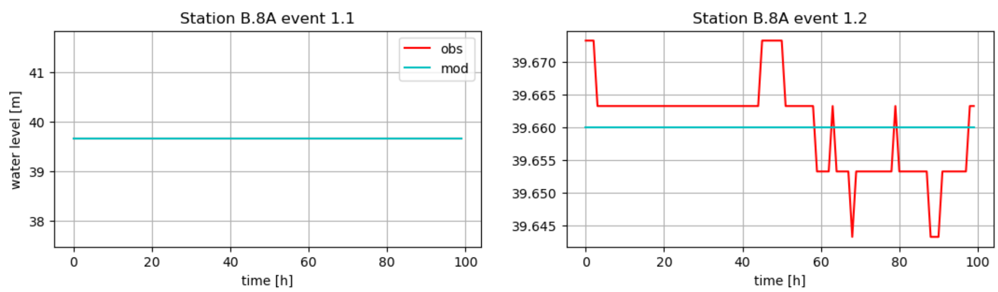

Figure 5.6: Hydrographs of the observed and modelled water levels in the Huai Phak river for event 1.1 and event 1.2.

5.2. River capacity

The discharge in the Phetchaburi river is decided by the reservoir dam outflows. To get an idea of how high these outflows can be before the Phetchaburi river starts to flood, the outflows of the reservoir dams were increased until the most vulnerable locations started to flood. Since the focus was on the maximum capacity of the Phetchaburi river for this part of the study, precipitation was not included as input. The only other variable was the Phet Diversion Dam outflow, for which there were two scenarios. The first one was the ”closed” scenario, the Phet Diversion Dam did not open further so the outflow stayed constant at a rate of 50 m^3/s throughout the whole run. The second one was the ”open” scenario, the water level at the Phet Diversion Dam stayed constant at a value of 18.3 m, which was the mean value for the years 2019 to 2023. The outflow of the Phet Diversion Dam could increase depending on the discharge in the Phetchaburi river. For simplicity, only the outflow of the Kaeng Krachan Dam, which discharges into the Phetchaburi river, was changed. The outflows from the Mae Prachan Dam and Huai Phak Dam stayed constant at a rate of 15 m^3/s and 5 m^3/s respectively.

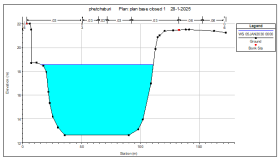

(a) Loc 1: closed, 55 m^3/s

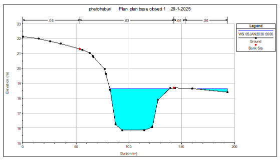

(b) Loc 2: closed, 55 m^3/s

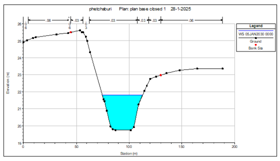

(c) Loc 3: closed, 55 m^3/s

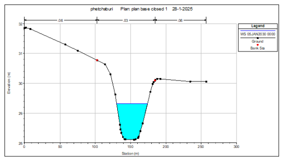

(d) Loc 4: closed, 55 m^3/s

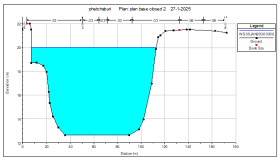

(e) Loc 1: closed, 120 m^3/s

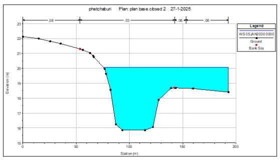

(f) Loc 2: closed, 120 m^3/s

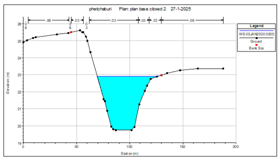

(g) Loc 3: closed, 120 m^3/s

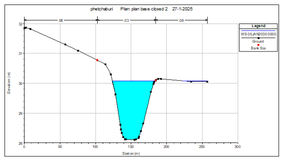

(h) Loc 4: closed, 120 m^3/s

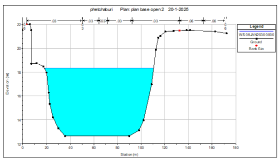

(i) Loc 1: open, 120 m^3/s

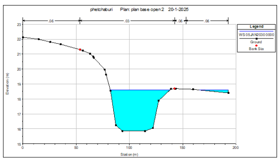

(j) Loc 2: open, 120 m^3/s

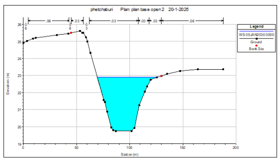

(k) Loc 3: open, 120 m^3/s

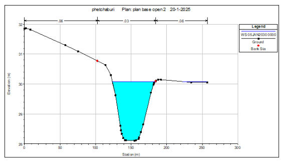

(l) Loc 4: open, 120 m^3/s

Figure 5.7: Water levels in the cross sections at locations 1, 2, 3 and 4 respectively from downstream to upstream on the Phetchaburi river for the closed and open scenarios for different discharges.

The results for the water levels can be seen in Figure 5.7. Each column is a cross section at a specific location (Appendix C) and from left to right it goes from downstream to upstream on the river. Location 1 is a cross section immediately upstream of the Phet Diversion Dam. The other locations were chosen based on where the Phetchaburi river is sensitive to floods. All these locations are on the lower half of the Phetchaburi river since the upper half does not experience any floods. For the closed scenario with an outflow of 35 m^3/s from the Kaeng Krachan Dam, which resulted in a total discharge of 55 m^3/s, the water level just reached the riverbank height at location 3. In case of the open scenario, this same water level was reached when the outflow from the Kaeng Krachan Dam was 100 m^3/s and thus a total discharge of 120 m^3/s. From downstream to upstream, at around one third of the Phetchaburi river the downstream condition had no effect on the upstream water levels any more, which was around location 3. From there on out the water levels in both scenarios were the same if the discharges were the same. The water level at location 3 is the same for both scenarios with a total discharge of 120 m^3/s and this is also the case for location 4 (Figure 5.7). However, at location 1 and 2 the water levels are much higher in the closed scenario for the same inflow.

5.3. Selecting and assessing infiltration parameters and precipitation data types

As explained in Chapter 3, part of the total amount of precipitation in the Phetchaburi river basin infiltrates into the subsurface and the remaining part becomes runoff. For the chosen infiltration method, which was the Deficit and Constant method, there were three parameters. The maximum deficit and initial deficit were set to a constant value of 20 mm and 10 mm respectively. For the percolation rate, which is the parameter that decides how fast precipitation infiltrates into the subsurface, there were four scenarios as described in Chapter 4:

- No infiltration: all the precipitation will end up in the river basin.
- Percolation rate of 3 mm/hr: the same value for every land use type.
- Percolation rate of 5 mm/hr: the same value for every land use type.
- Percolation rate varying from 5 to 20 mm/hr: every forest land use type has a percolation rate of 20 mm/hr, all else has a percolation rate of 5 mm/hr.

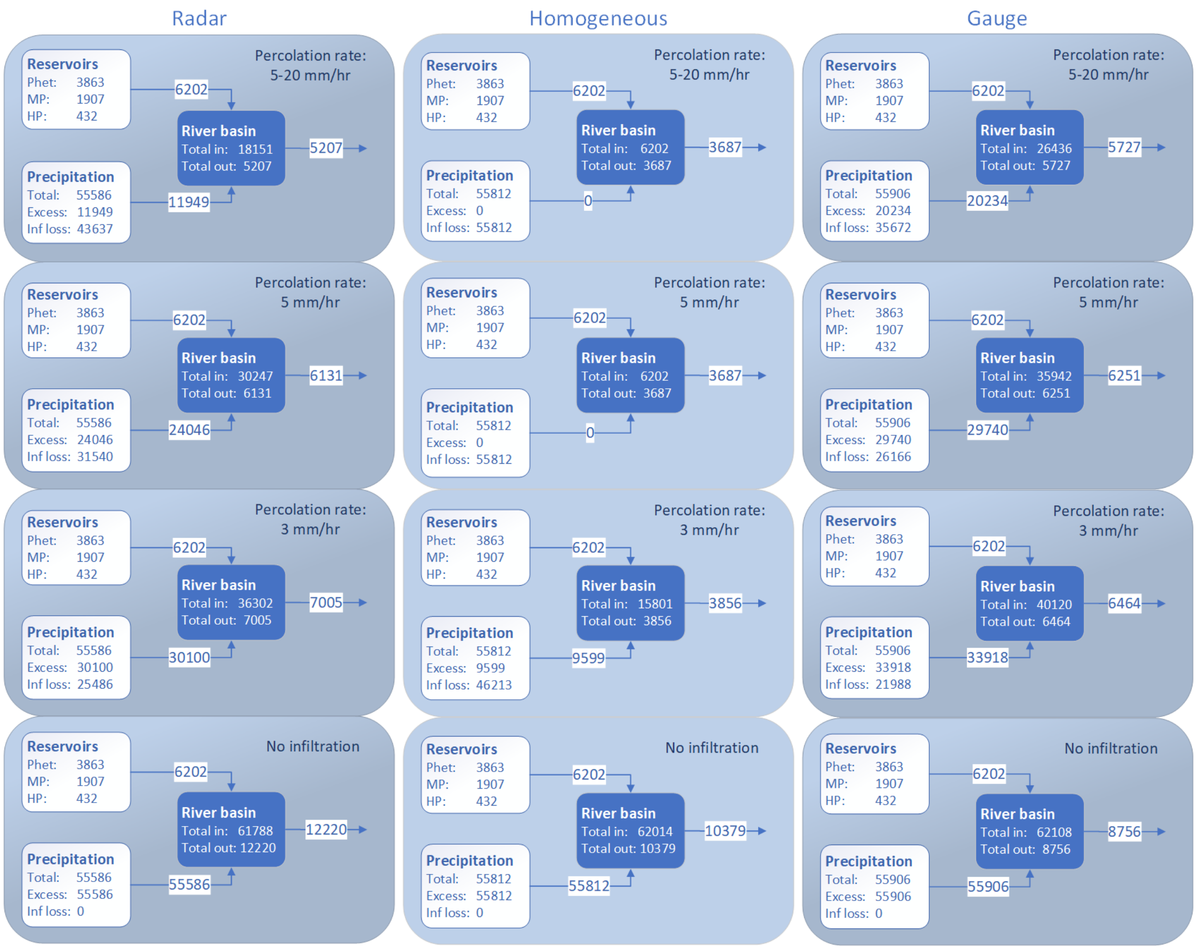

Figure 5.8: Water balance diagrams for each infiltration and precipitation data type scenario for event 2.1 in 1000 m^3. For the radar and gauge scenarios an increase in the percolation rate results in similar decrease in precipitation excess while the homogeneous scenarios result in little to no excess precipitation.

The four infiltration scenarios combined with the three precipitation scenarios resulted in a total of twelve scenarios, and thus twelve water balances, for each event. In each water balance diagram (Figures 5.8 and 5.9), the upper white box shows the amount of water coming from each reservoir and the lower white box shows the total amount of precipitation, the excess precipitation and the infiltration loss. The arrows show the total values from the reservoirs, the total precipitation that enters the river basin, and the amount of water that leaves the system through the Phet Diversion Dam. For each scenario the total precipitation stayed the same while the infiltration loss, and therefore also the excess precipitation, changed.

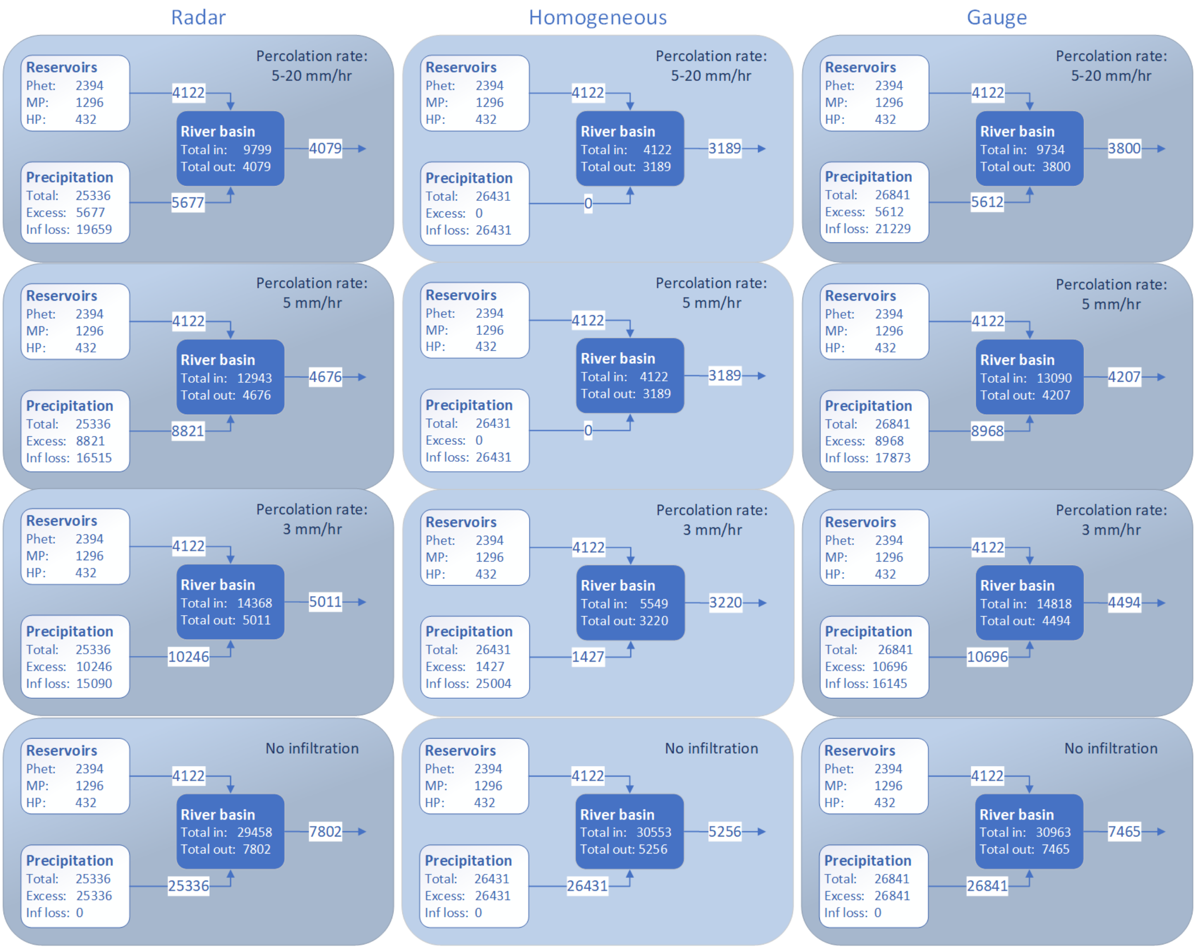

Figure 5.9: Water balance diagrams for each infiltration and precipitation data type scenario for event 2.2 in 1000 m^3. For the radar and gauge scenarios an increase in the percolation rate results in similar decrease in precipitation excess while the homogeneous scenarios result in little to no excess precipitation.

In every scenario when the percolation rate increases, more water can infiltrate into the subsurface and thus the infiltration loss increases and excess precipitation decreases. It is noticeable that when homogeneous precipitation data is used as input, the excess precipitation already becomes around 17% of the total precipitation with a small infiltration rate for event 2.1 and around 5% for event 2.2. With a small increase in the infiltration rate the excess precipitation even goes to zero. Using homogeneous precipitation data in the highest infiltration scenario also results in the excess precipitation being zero. When spatially distributed precipitation data from the weather radar or rain gauges is used as input, the decrease in excess precipitation is less steep. For the highest infiltration scenario the excess precipitation is around 21% and 36% of the total precipitation for event 2.1 for weather radar and rain gauges respectively. For event 2.2 this is around 20% of the total precipitation for both weather radar and rain gauges. It is noticeable that when precipitation data from weather radar is used as input, the resulting water balances are very similar to the water balances resulting from using precipitation data from rain gauges as input.

Table 5.4: Bias of the modelled water levels in the Phetchaburi river and its tributaries for event 2.1 and 2.2.

Station	Bias event 2.1 [m]	Bias event 2.2 [m]
B.3A	-0.11	-0.09
B.9	0.15	-0.08
B.11	0.07	-0.11
B.6A	-0.55	0.2
B.8A	0	0.13

For each of the twelve scenarios, there are five telemetering stations with water levels for both events (Appendix D). The measured water levels were visually corrected for a bias (Table 5.4) so that the base water level was the same for both the modelled and measured water levels. In this section certain stations are highlighted (Figures 5.10 to 5.14). For each station, the upper three plots show for each precipitation data type the water levels for each infiltration scenario. This way it can be seen how the water level reacts when infiltration into the subsurface increases. The lower plots contain the same results, but plotted differently to highlight what the effect of each type of precipitation data on the water levels is and how they compare to each other. In each plot there is an extra result for a scenario with no precipitation so the distinction can be made between an increase in water level caused by precipitation or an increased reservoir dam outflow.

Table 5.5: RMSE of the modelled water levels at station B.3A upstream on the Phetchaburi river for event 2.1.

Scenario	Radar RMSE [m]	Homogeneous RMSE [m]	Gauge RMSE [m]
No infiltration	0.330	0.268	0.159
Perc rate 3 mm/hr	0.157	0.086	0.099
Perc rate 5 mm/hr	0.132	0.080	0.092
Var perc rate	0.095	0.080	0.083

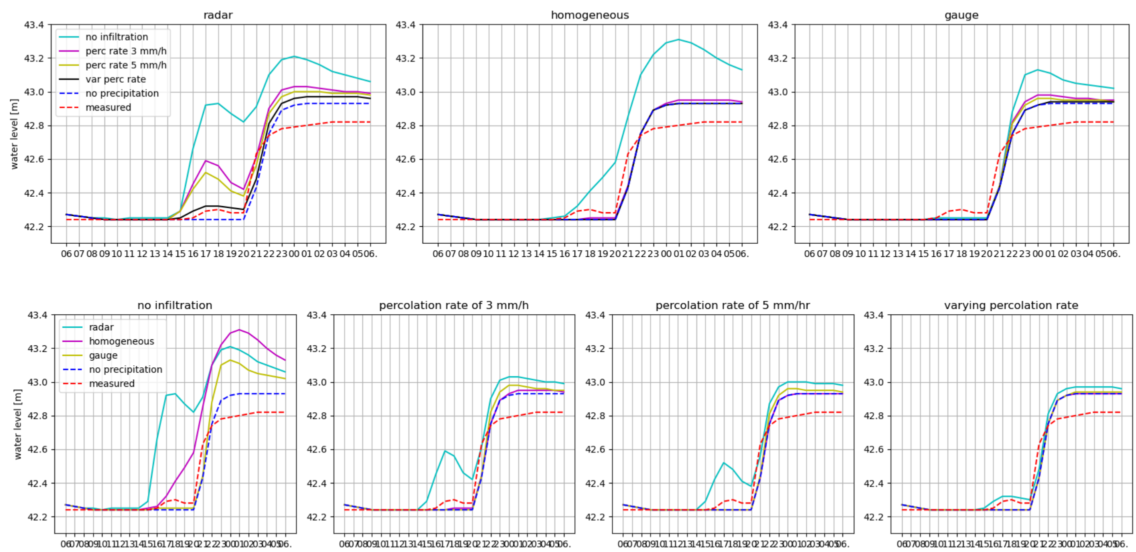

Figure 5.10: Water levels for each infiltration and precipitation data type scenario at station B.3A upstream on the Phetchaburi river for event 2.1.

In the measured water level during event 2.1 at station B.3A, which is the most upstream telemetering station on the Phetchaburi river, a small peak in the water level followed by a big rise in the water level are visible (Figure 5.10). The big rise in the water level is caused by an increase in reservoir outflow since it can also be observed in the water levels in the scenario without precipitation. For the modelled water levels, the small peak in the water level is only present in the water levels modelled with weather radar precipitation data as input. It is also not present in the water level modelled without precipitation, which indicates that it is not caused by reservoir outflow. The RMSE are smallest for the scenarios with homogeneous precipitation data input where all the precipitation infiltrated into the subsurface and no excess precipitation was present (Table 5.5). This suggests that precipitation does not play a significant role in this case and using only reservoir outflow the water level can already be properly modelled.

Table 5.6: RMSE of the modelled water levels at station B.9 downstream on the Phetchaburi river for event 2.1.

Scenario	**Radar RMSE [m]**	**Homogeneous RMSE [m]**	**Gauge RMSE [m]**
No infiltration	0.657	0.777	0.859
Perc rate 3 mm/hr	0.230	0.078	0.589
Perc rate 5 mm/hr	0.158	0.097	0.527
Var perc rate	0.054	0.097	0.364

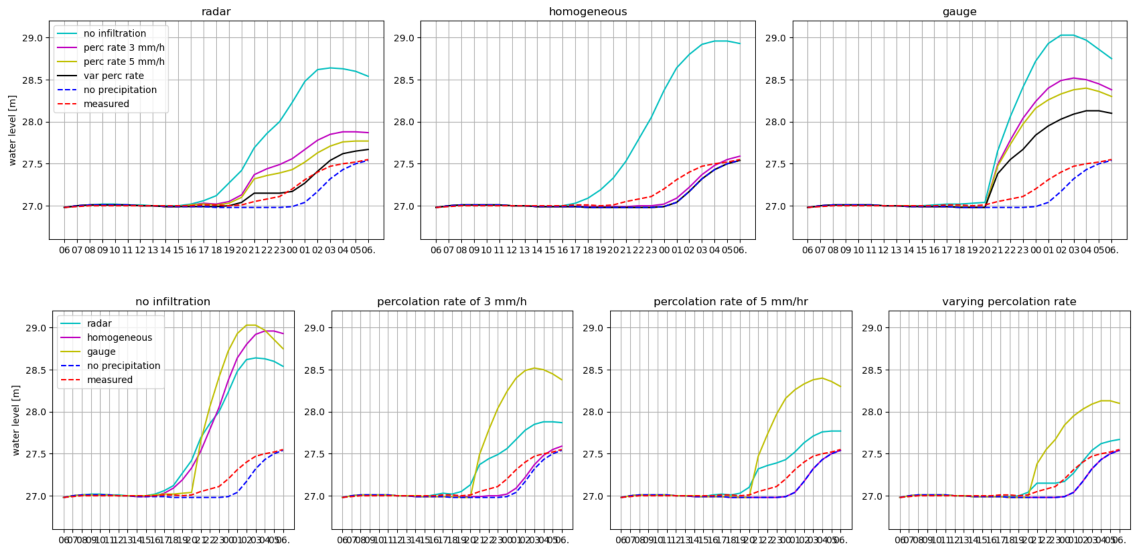

Figure 5.11: Water levels for each infiltration and precipitation data type scenario at station B.9 downstream on the Phetchaburi river for event 2.1.

In most cases, using precipitation data from weather radar as input results in the highest water levels. This is however not the case for station B.9 during event 2.1 (Figure 5.11). Using precipitation data from the rain gauges as input results in high water levels for station B.9, even for the highest infiltration scenario, and this also results in high RMSE values (Table 5.6). As for using homogeneous precipitation data as input, here again the infiltration scenarios that lead to no excess precipitation result in water levels that are quite close to the measured water levels, but in this case they are slightly underestimating the water levels. Using precipitation data from weather radar in combination with the highest infiltration scenario with varying percolation rates results in a bit of excess precipitation. This results in slightly higher water levels and a smaller RMSE than in the case of using homogeneous precipitation data as input where there is no excess precipitation at all.

Table 5.7: RMSE of the modelled water levels at station B.6A downstream on the Mae Prachan river for event 2.1.

Scenario	**Radar RMSE [m]**	**Homogeneous RMSE [m]**	**Gauge RMSE [m]**
No infiltration	1.184	0.669	0.327
Perc rate 3 mm/hr	0.398	0.603	0.547
Perc rate 5 mm/hr	0.222	0.634	0.592
Var perc rate	0.167	0.634	0.617

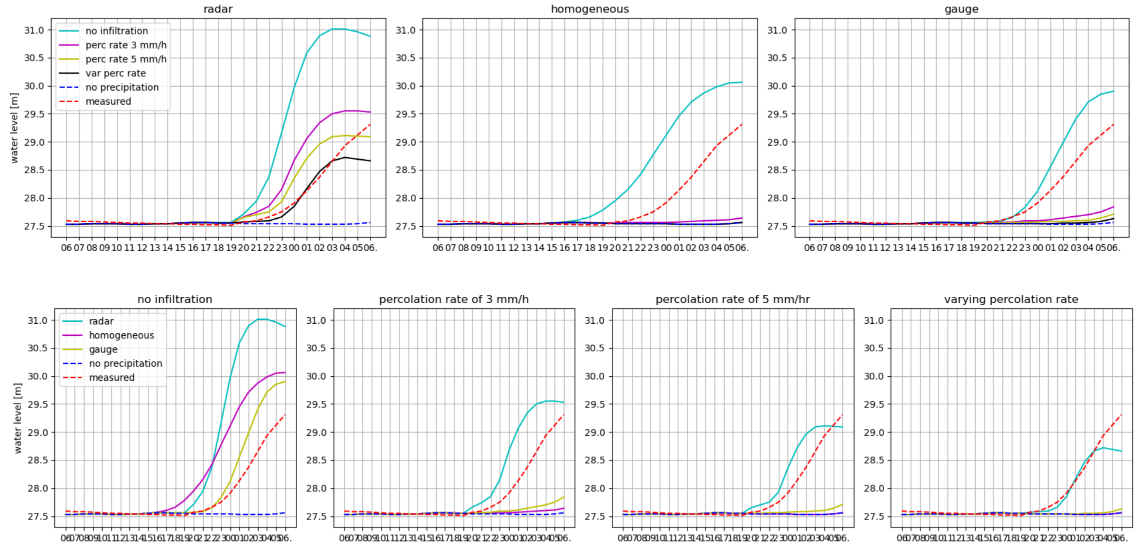

Figure 5.12: Water levels for each infiltration and precipitation data type scenario at station B.6A downstream on the Mae Prachan river for event 2.1.

Station B.6A during event 2.1 (Figure 5.12) is an example of a case where a big increase in water level is not caused by an increase in reservoir dam outflow. The big increase in the measured water level is not present in the modelled water levels without precipitation, which indicates that the increase in water level is caused by precipitation. When homogeneous precipitation data is used as input, the water level does not increase when infiltration is included, even for the smallest percolation rate. When precipitation data from rain gauges is used as input, the water level slightly increases but this is almost negligible. Using both these types of precipitation data as input thus underestimates the water level, which can also be seen from the high RMSE for these scenarios (Table 5.7). Only when precipitation data from weather radar is used as input, the big increase in water level is present. When no infiltration is present and all the precipitation becomes runoff, the water level is overestimated. The best result with the smallest RMSE is when infiltration is varied, with a high percolation rate for forest land.

Table 5.8: RMSE of the modelled water levels at station B.3A upstream on the Phetchaburi river for event 2.2.

Scenario	**Radar RMSE [m]**	**Homogeneous RMSE [m]**	**Gauge RMSE [m]**
No infiltration	0.343	0.172	0.133
Perc rate 3 mm/hr	0.211	0.114	0.113
Perc rate 5 mm/hr	0.191	0.113	0.114
Var perc rate	0.123	0.113	0.113

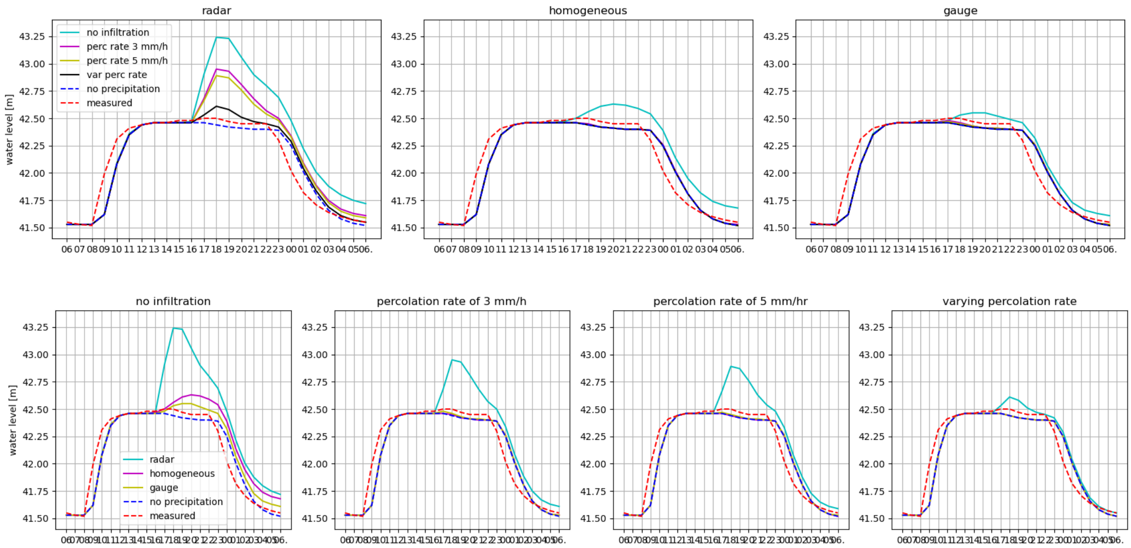

Figure 5.13: Water levels for each infiltration and precipitation data type scenario at station B.3A upstream on the Phetchaburi river for event 2.2.

At station B3.A during event 2.2 there is an increase in the measured water level (Figure 5.13). This increase is also present in the modelled water level for the scenario without precipitation, indicating that the increase in water level is caused by an increase in reservoir dam outflow. Using homogeneous precipitation data as input results in modelled water levels similar to the measured water levels. This is also the case when precipitation data from rain gauges is used as input and the RMSE for both these precipitation data types are also similar (Table 5.8). When precipitation data from weather radar is used however, an additional peak on top of the increased water levels can be observed, contrary to the measured water level. Only when infiltration into the subsurface increases does the modelled water level come closer to the measured water level. This can also be observed from the RMSE, which gets smaller the higher the percolation rate becomes.

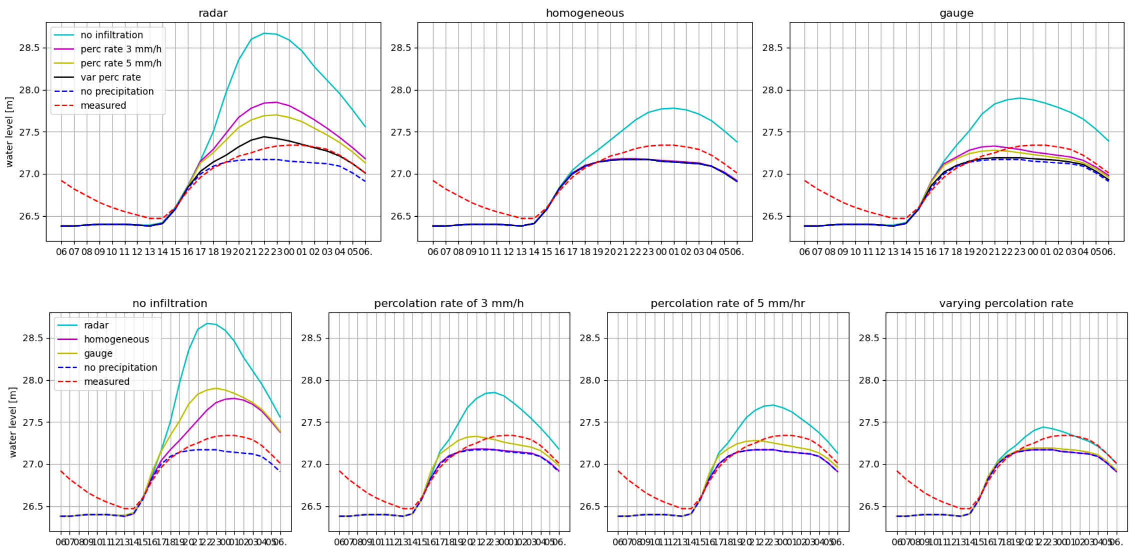

Figure 5.14: Water levels for each infiltration and precipitation data type scenario at station B.9 downstream on the Phetchaburi river for event 2.2.

Table 5.9: RMSE of the modelled water levels at station B.9 downstream on the Phetchaburi river for event 2.2.

Scenario	**Radar RMSE [m]**	**Homogeneous RMSE [m]**	**Gauge RMSE [m]**
No infiltration	0.798	0.341	0.426
Perc rate 3 mm/hr	0.360	0.151	0.171
Perc rate 5 mm/hr	0.293	0.152	0.163
Var perc rate	0.176	0.152	0.150

At station B.9 during event 2.2 all the precipitation scenarios without infiltration result in modelled water levels that are higher than the measured water levels. When infiltration is included when homogeneous precipitation data is used as input, the water level goes down to the same water level as the scenario without precipitation. When precipitation data from rain gauges is used, the water level resembles the measured water levels when infiltration is included, however, for the highest infiltration scenario the water level also goes down to the same water level as the scenario without precipitation. When precipitation data from weather radar is used as input, the water levels go down when infiltration is included, but not as low as for the other precipitation data types. The water level only comes close to the measured water level for the highest infiltration scenario. The RMSE for both homogeneous precipitation data and rain gauge precipitation data are already quite low for the scenarios with infiltration, but for weather radar precipitation data it only becomes low for the scenario with varying percolation rates Table 5.9.

6 Discussion

6.1. Model and data limitations

There are several limitations in the model caused by lack of data. For the DEM the quality and accuracy are more important than the resolution and precision (Ali et al., 2015). The DEM available for this study had a quite high resolution of 5 m, however it was old and a DEM also does not capture river depth, so the cross sections taken directly from the DEM for the 1D component needed modifications. Cross section data was available, however all the cross sections were 3 km or more apart. The model needed cross sections every 200 m or less to be stable but using interpolation resulted in unrealistic cross sections. All cross sections in the model were thus modified and interpolated by hand based on the cross section data. As a result, the river bathymetry in the river might not everywhere be completely the same as the actual river bathymetry.

In the model, the Manning's roughness coefficient does not vary along the river for simplicity. In reality, the roughness coefficient does vary. A study by de Doncker et al. (2009) shows that the Manning's roughness coefficient can vary over the year as the amount of vegetation changes during the year and even accidental obstacles can influence it. Since Thailand is in a tropical region, the vegetation does not go through any seasonal changes. However, the amount of vegetation in the downstream part of the Phetchaburi river and Mae Prachan river is much more than more upstream (Figure 6.1). There are plans to remove vegetation from the Phetchaburi river so the Manning's roughness coefficient might need to be changed in the future. A study by Attari and Hosseini (2019) presented a new method that is able to calibrate the river with different Manning's roughness coefficients for different parts of the river.

For the Mae Prachan river and Huai Phak river, the outflow of the reservoir for irrigation goes to a separate irrigation channel. However, for the Phetchaburi river the outflow meant for irrigation goes into the main river itself. In case water is taken from the river for irrigation, it is thus possible that the discharge in the river due to reservoir outflow can decrease. However, this was not taken into account in this study.

As mentioned before, only daily data of the outflow of the Mae Prachan Dam and Huai Phak Dam were available so these rivers could not be calibrated on wave celerity. On top of this, the outflow data that was available contained a lot of low outflows, however the model runs into stability issues for low flows, especially in combination with low Manning's roughness coefficients. For the Mae Prachan river this did not result in any noticeable problems. For the Huai Phak river however, the modelled peak is a few hours too early compared to the measured peak (Figures D.5 and D.10).

(a) Phetchaburi river downstream (just upstream of Phet Diversion Dam). A lot of vegetation covering half the river.

(b) More upstream on the Phetchaburi river there is no vegetation covering the river any more.

(c) A lot of vegetation downstream in the Mae Prachan river, making the river itself barely visible.

Figure 6.1: Photos of the Phetchaburi river and Mae Prachan river.

6.2. The Phetchaburi river basin without precipitation

In case the water level right upstream of the Phet Diversion Dam is maintained at a regular water level and the Phet Diversion Dam outflow thus increases with the discharge, the river can handle around a total discharge of 120 m^3/s before it starts flooding at the most vulnerable locations of the study area. If the Phet Diversion Dam is not fully open and instead a regular outflow of 50 m^3/s is maintained, the threshold for the total discharge in the river is around 55 m^3/s before it starts flooding downstream (upstream of the Phet Diversion Dam). The upstream part only floods when the discharge is increased to 120 m^3/s. The Phet Diversion Dam is thus crucial for floods in the downstream part of the middle reach of the Phetchaburi river.

6.3. The Phetchaburi river basin with precipitation

Infiltration

Infiltration plays a significant role when precipitation falls in the river basin. The amount of precipitation that infiltrates into the subsurface ends up in the groundwater, which is out of the scope of this study. The remaining precipitation becomes surface runoff in the river basin. For the scenario with the best results, around 80% of the precipitation was infiltrated into the subsurface and thus only 20% of the precipitation resulted in runoff. This is the scenario where the percolation rate was high for forest areas and low for non-forested areas. A study by Mongil-Manso et al. (2025) shows that forest cover increases soil infiltration, with a pine forest having an infiltration rate of five times higher than a scrubland. Other studies have also concluded that infiltration is affected by land use (Schwartz et al., 2003; Bormann and Klaassen, 2008; Liu et al., 2018). In this study it was decided to use a simple type of infiltration method, namely the Deficit and Constant method. However, more complex infiltration methods exist and different infiltration methods can lead to different results (Chahinian et al., 2005). HEC-RAS can also use the SCS Curve Number method and the Green-Ampt method, however these methods require more parameters.

Even though a large fraction of the precipitation infiltrated into the subsurface, the amount of precipitation that did end up in the river is still high, resulting in high outflows. From the measured outflow data of the Phet Diversion Dam an estimation was made of the amount of water leaving the system, for event 2.1 this was around 4320000 m^3 and for event 2.2 around 2765000 m^3. Compared to these river outflows, the modelled river outflows (Figures 5.8 and 5.9) are in most scenarios higher. For event 2.2, the scenarios that had homogeneous precipitation data as input and a percolation rate of 5 mm/hr or higher have no excess precipitation but even then the modelled river outflows are too high. To find the cause of these differences, rating curves were plotted for each telemetering station in the rivers (Figures 6.2 to 6.5). For most stations a higher discharge is needed for the model to reach the same water level as the measured ones, especially for the Mae Prachan river (Figure 6.3). This might explain why the modelled outflows are bigger than the measured ones since the rivers are calibrated on water level. Aside from the bias in the water levels, the trends of the modelled rating curves seem to be similar to the trends of the measured rating curves in most cases, except for the Huai Phak river (Figure 6.5).

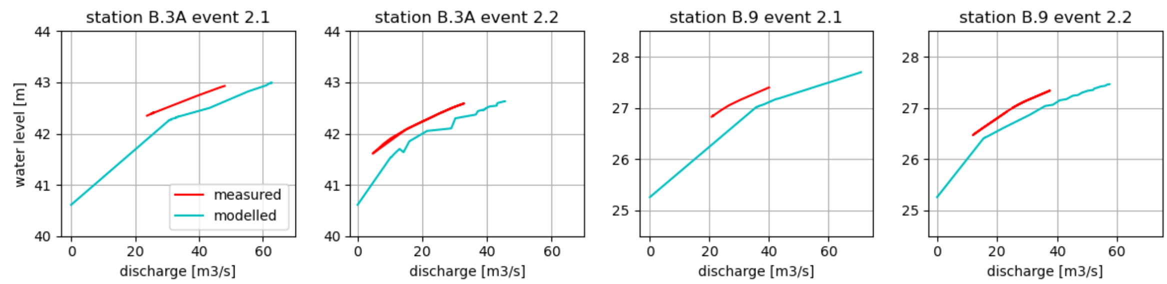

Figure 6.2: Rating curves for station B.3A (upstream) and B.9 (downstream) on the Phetchaburi river.

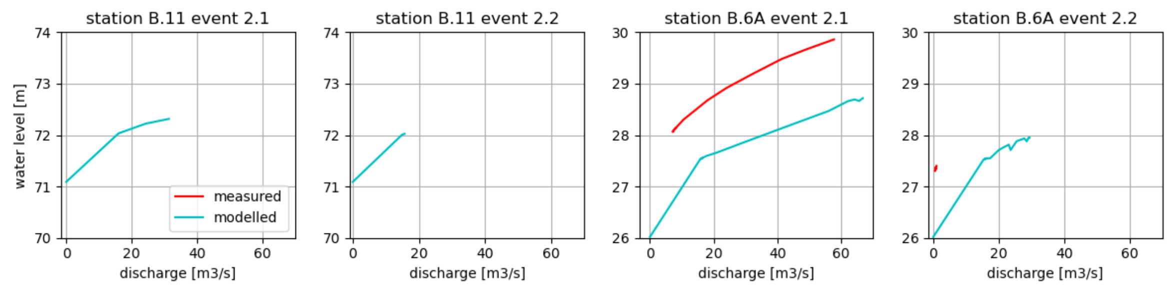

Figure 6.3: Rating curves for station B.11 (upstream) and B.6A (downstream) on the Mae Prachan river.

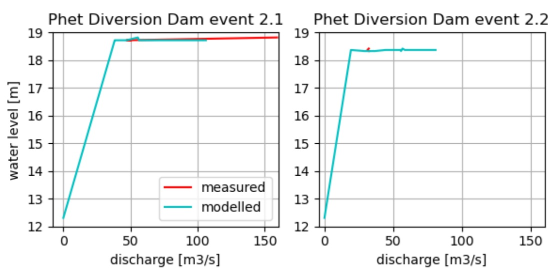

Figure 6.4: Rating curves for the Phet Diversion Dam, just upstream of the dam.

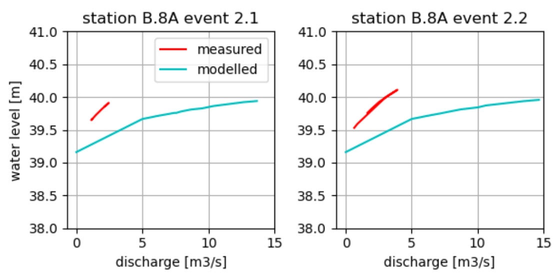

Figure 6.5: Rating curves for station B.8A on the Huai Phak river.

When no infiltration is present in the study area, the modelled water levels are significantly higher than the measured water levels for most stations, regardless of the precipitation data type. When infiltration is included in the study area, the results for the modelled water levels are different for each precipitation data type. When precipitation data from weather radar is used as input, the water level significantly goes down when infiltration is included. The water levels do not go down completely as the peaks in the water levels can still be seen for every infiltration scenario, with small but noticeable differences. When the input is homogeneous precipitation data, the water level goes down completely already for the lowest infiltration scenario and no peaks can be observed for both events regardless of the station. The precipitation intensity is too low and thus never exceeds the soil infiltration capacity, leading to no surface runoff and no peaks in the water level. A study by Arnaud et al. (2002) compared uniform and non-uniform precipitation and found similar results, for the model that only produces runoff after the cumulative precipitation exceeds a certain threshold, using uniform precipitation input results in an underestimation of peak flows and runoff volumes. A study by Nicótina et al. (2008) suggests that when infiltration excess mechanisms are important in quite large basins, the spatial distribution of precipitation might play an important role. In my study the only contribution to the runoff aside from the reservoir outflows is excess precipitation, which explains why infiltration has a big influence on runoff and water levels.

Spatially distributed precipitation

In this section the focus is on the results obtained with the infiltration scenario with a percolation rate of 20 mm/hr for forest land and a percolation rate of 5 mm/hr for all else. Using these percolation rates lead to the highest amount of infiltration into the subsurface and this lead to the best water level results. As discussed in the previous section, using homogeneous precipitation data lead to poor results as no excess precipitation was produced. When it comes to spatially distributed precipitation, using precipitation data from rain gauges as input lead to mixed results. At some stations there is no peak in the water level where there should be one, while at some stations the peak in the water level is overestimated. This can be explained by the density of the rain gauges and the way they are interpolated. A high amount of total accumulated precipitation can be seen in the south as a result of the precipitation measured by the rain gauges during event 2.1 (Figure 6.6b), which is not present in the total amount of accumulated precipitation as a result of precipitation measured by the weather radar (Figure 6.6a). The only two rain gauges available in the south for this time period were stations STN0480 and PCH003 (Figure 2.13). They are close to each other and both registered high precipitation values. Since there are no other stations in the south, the whole area is interpolated to have a high amount of precipitation, while for the weather radar there is less precipitation accumulated further south. As a result, the water levels at telemetering station B.9 (Figure 5.11) end up being higher when precipitation data from rain gauges is used as input.

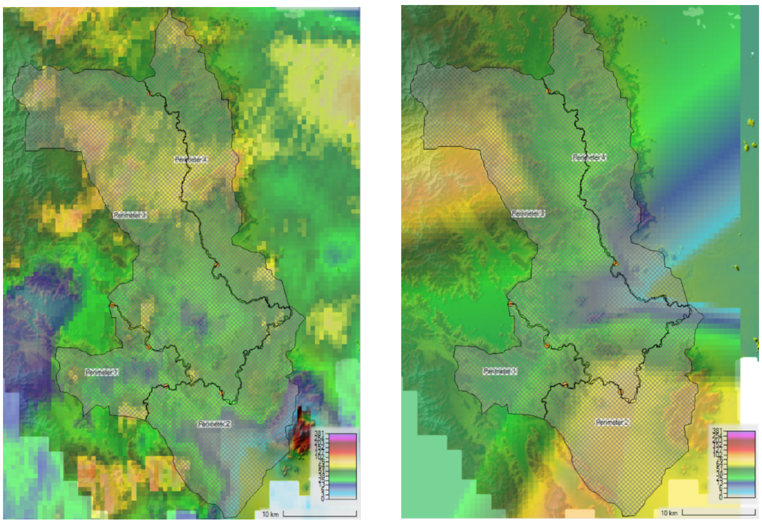

(a) Weather radar precipitation data   (b) Interpolated rain gauge precipitation data

Figure 6.6: Total accumulated precipitation in the study area at the end of precipitation event 2.1 for the two spatially distributed precipitation data type inputs. The study area is highlighted by the mesh and only precipitation inside these boundaries are taken into account.

The opposite also happened during the same event, for example for telemetering station B.6A the peak in the water level completely disappears when using precipitation data from rain gauges as input, just like when homogeneous precipitation data is used as input (Figure 5.12). This can also be seen when looking at the total amount of accumulated precipitation in the north, the precipitation event that can be observed in yellow for weather radar is not present for the rain gauges (Figure 6.6). In this area there are no rain gauges, so the precipitation that is detected by the weather radar does not get detected by the rain gauges.

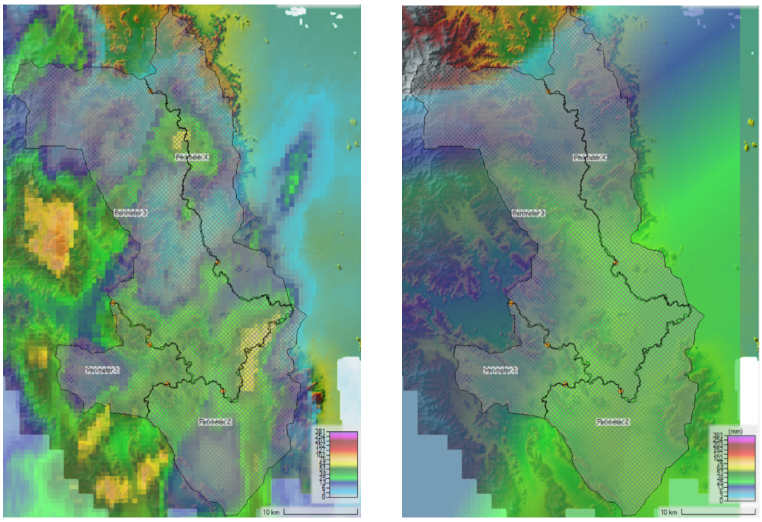

(a) Weather radar precipitation data

(b) Interpolated rain gauge precipitation data

Figure 6.7: Total accumulated precipitation in the study area at the end of precipitation event 2.2 for the two spatially distributed precipitation data type inputs. The study area is highlighted by the mesh and only precipitation inside these boundaries are taken into account.

Another disadvantage of interpolated precipitation data from rain gauges is that when the Thiessen polygon method is used, information from adjacent rain gauge stations are often ignored which results in a precipitation surface that is not continuous (Guo et al., 2022). In this study it was decided to use the Thiessen polygon method to interpolate precipitation data from the rain gauges, but in HEC-RAS it is also possible to use the Inverse Square of the Distance method, the Inverse Distance Squared (Restricted) method and the Peak Preservation method. However, these are all statistical interpolation methods. Geostatistical interpolation methods on the other hand use additional information, like elevation, for more accurate estimation of the precipitation and these methods seem to perform better most of the time (Goovaerts, 2000; Lloyd, 2005; Haberlandt, 2007; Pellicone et al., 2018). However, a study by Sun et al. (2025) modelled flash floods with around the same amount of rain gauges as in my study but for a smaller region and found that the Thiessen polygon method gave proper results while the results for the uniform method were not satisfactory at all.

As for spatially distributed precipitation data from weather radar, using these in the Phetchaburi river basin results in visible peaks in the water level, even when the amount of precipitation lost to infiltration into the subsurface is high. A downside of raw weather radar products is that they are in the form of reflectivity and contain a lot of errors so a conversion to precipitation rates and a lot of corrections are needed (Chumchean et al., 2003; Berne and Uijlenhoet, 2006). The radar data for this study was converted and corrected and it is interesting to see that these can perform well in modelling water levels in the Phetchaburi river. A study by Loritz et al. (2021) found that especially for storms with high spatio-temporal variabilities the model performance improved when using spatially distributed precipitation as input in a hydrological model.

Despite the differences in spatial variability between precipitation data obtained from weather radar and precipitation data obtained from rain gauges, they perform quite similarly when solely looking at the water balance results. This shows that even if the total water fluxes in and out of the Phetchaburi river basin are in the right order, this would not be sufficient information to describe the floods. The spatial variability of precipitation is crucial for modelling floods at the right location. To highlight this effect, two cross sections were chosen to visualise the difference in the water level when using one or the other type of spatially distributed precipitation data (Figures 6.8 and 6.9). As mentioned before, a big precipitation event was observed in the north during event 2.1 when looking at the precipitation data from weather radar and this resulted in water levels with the smallest RMSE, while using precipitation data from rain gauges did not have this result (Table 5.7). When looking at a cross section of the Mae Prachan river in this area (Figure 6.8) it can be seen that using precipitation data from weather radar leads to flooding, while using precipitation data from rain gauges does not. Assuming the water level obtained with precipitation data from weather radar as input is the correct one based on RMSE, this means that using precipitation data from rain gauges as input underestimates the water level in the river and incorrectly leads to no flooding. Similarly when looking at the south for the same precipitation event, using precipitation data from weather radar leads to the smallest RMSE in the water levels so these can be representative of the reality (Table 5.6). When looking at a cross section of the Phetchaburi river (Figure 6.9), using precipitation data from rain gauges as input leads to flooding while using precipitation data from weather radar does not. In this case using precipitation data from rain gauges incorrectly leads to flooding.

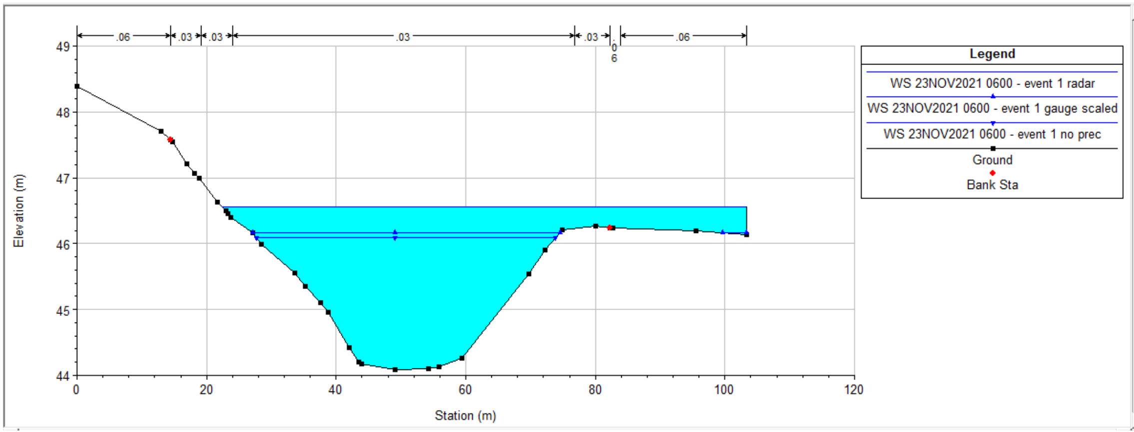

Figure 6.8: Water levels for different precipitation data types in a cross section of the Mae Prachan river at the end of precipitation event 2.1. Lowest line is the water level without precipitation. Using precipitation data from weather radar leads to a flood while using precipitation data from rain gauges does not.

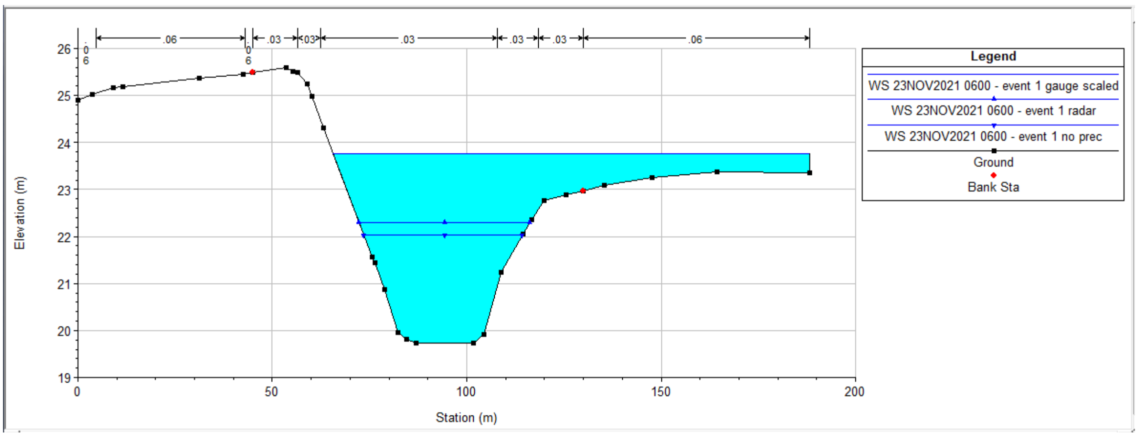

Figure 6.9: Water levels for different precipitation data types in a cross section of the Phetchaburi river at the end of precipitation event 2.1. Lowest line is the water level without precipitation. Using precipitation data from rain gauges leads to a flood while using precipitation data from weather radar does not.

For both these locations the total amount of precipitation over a time period of a day that lead to flooding was around 80 mm in the surrounding area. The Phetchaburi river basin has experienced daily precipitation amounts of this size or bigger a few times a year for the years 2018-2022 (Appendix B). This is in line with the fact that the area experiences floods at least once a year.

However, while using precipitation data from weather radar leads to the best results overall, it does not always lead to perfect results. When it comes to precipitation event 2.2, which is a smaller precipitation event than precipitation event 2.1, using precipitation data from weather radar sometimes leads to an overestimation of the water level in the river. This is most prominent for station B.6A (Figure D.9) and it can be seen that using precipitation data from rain gauges as input here even leads to a better result. The cause of the peak in the water level is a small area where around 70 mm of precipitation had fallen in a day, which is the yellow area on the Mae Prachan river in Figure 6.7a. These precipitation peaks only lead to a quick increase in the water level for a time period of a few hours before going down again and also do not lead to any floods. While there are small spots of high precipitation, the amount is not enough for flooding. In the total amount of accumulated precipitation data obtained from rain gauges, the maximum precipitation amount is around 30 mm over a large area (Figure 6.7b). These kind of precipitation events generally do not cause stream floods.

7

Conclusions and recommendations

7.1. Conclusion

The aim of this study was to find an answer to the following question:

What is the effect of spatially distributed precipitation on the flooding of the middle reach of the Phetchaburi river?

To find an answer to this question, a combined 1D/2D model of the Phetchaburi river basin was made in HEC-RAS. Three different types of precipitation data were used, namely gridded data from a weather radar station, interpolated point data from automatic rain gauge stations and artificial homogeneous precipitation data. This research showed that the spatial variability of precipitation matters in the Phetchaburi river basin as the different types of precipitation data lead to different results despite the total amount of precipitation being the same for every scenario.

The cause of the big differences was the high infiltration rates in the study area. This study found that a large fraction of the precipitation infiltrates into the soil in the Phetchaburi river basin. When homogeneous precipitation data was used as input, precipitation intensity would be too low, allowing all precipitation to infiltrate into the subsurface. As a consequence no runoff was produced which lead to no increase in the river discharge and water levels. On the contrary, when spatially distributed precipitation data was used as input, precipitation intensities were high enough to exceed the soil infiltration capacity. This lead to surface runoff and stream floods.

When it comes to spatially distributed precipitation in the Phetchaburi river basin, both rain gauges and weather radar are available. When precipitation data from weather radar was used as input, the resulting water balances were similar to the ones obtained when precipitation data from rain gauges was used as input. On the other hand, the water balances obtained from using homogeneous precipitation data as input were completely different, except for the scenario without infiltration. When it comes to the total water volumes, the type of precipitation data does not matter much as long as it is spatially distributed. However, getting the correct volumes alone is not sufficient, for flood modelling it is also important that the modelled floods take place at the right locations. This is where detailed spatial variability of precipitation becomes important. The density of the rain gauge network in this area is too low to capture the spatial variability of the precipitation events in detail. This resulted in floods or the lack thereof at the wrong locations. Weather radar captures the spatial variability of precipitation in greater detail than rain gauges can. This study showed that using precipitation data from weather radar as input results in more accurate flood modelling in the Phetchaburi river basin.

Aside from precipitation, the discharge in the rivers is decided by the outflows of the reservoir dams and the outflow of the Phet Diversion Dam. The Phetchaburi river is sensitive to flooding when the Phet Diversion Dam is closed.

7.2. Recommendations

For flood modelling in the Phetchaburi river basin it is not recommended to use homogeneous precipitation data as this would highly underestimate floods. It is recommended to use spatially distributed precipitation data obtained from weather radar as this is more detailed than precipitation data obtained from rain gauges.

In this study the focus was on the effect of precipitation on the flooding of the middle Phetchaburi river basin. However, the study area has three reservoir dams upstream and the Phet Diversion Dam downstream. These dam outflows influence the discharges in the Phetchaburi river and its tributaries and these can be controlled. For further studies it would thus be interesting to research what the effect of precipitation in combination with management of the reservoir dams and the Phet Diversion Dam is on the flooding of the Phetchaburi river. Several questions that could be researched are:

- When there is a forecasting of a precipitation event, can floods be prevented by pre-emptively lowering the reservoir dam outflows?
- When a precipitation event is happening, can increasing the Phet Diversion Dam outflow still prevent or reduce floods?
- Can the Phet Diversion Dam outflow be increased during extreme events without causing floods downstream of the Phet Diversion Dam?
- What happens to the floods in the Phetchaburi river basin if extreme precipitations increase in intensity because of climate change?

To improve the model, it is recommended to monitor water levels and discharge at the Phet Diversion Dam on at least an hourly basis so that the downstream boundary condition is more accurate. The model could also not be properly calibrated for the Mae Prachan river and Huai Phak river because the temporal resolution of the reservoir outflow data was not high enough. To improve the calibration of these rivers, and thus better characterize these rivers, it is recommended to look into obtaining at least hourly reservoir outflow data.

Bibliography

Ali, A. M., Solomatine, D. P., & Baldassarre, G. D. (2015). Assessing the impact of different sources of topographic data on 1-D hydraulic modelling of floods. *Hydrology and Earth System Sciences*, *19*(1), 631–643. https://doi.org/10.5194/hess-19-631-2015

Arnaud, P., Bouvier, C., Cisneros, L., & Dominguez, R. (2002). Influence of rainfall spatial variability on flood prediction. *Journal of Hydrology*, *260*(1-4), 216–230. https://doi.org/10.1016/S0022-1694(01)00611-4

Asadieh, B., & Krakauer, N. Y. (2017). Global change in flood and drought intensities under climate change in the 21st century. *Hydrology and Earth System Sciences*. https://doi.org/10.5194/tc-2018-95

Attari, M., & Hosseini, S. M. (2019). A simple innovative method for calibration of Manning's roughness coefficient in rivers using a similarity concept. *Journal of Hydrology*, *575*, 810–823. https://doi.org/10.1016/j.jhydrol.2019.05.083

Bárdossy, A., & Pegram, G. (2013). Interpolation of precipitation under topographic influence at different time scales. *Water Resources Research*, *49*(8), 4545–4565. https://doi.org/10.1002/wrcr.20307

Barkau, R. L. (1982). Simulation of the July 1981 Flood Along the Salt River [Report for CE695BV, Special Problems in Hydraulics, Department of Civil Engineering, Colorado State University, Ft. Collins, CO.].

Berne, A., & Uijlenhoet, R. (2006). Quantitative analysis of X-band weather radar attenuation correction accuracy. *Natural Hazards and Earth System Sciences*, *6*, 419–425. https://doi.org/10.5194/hess-14-205-2010

Bormann, H., & Klaassen, K. (2008). Seasonal and land use dependent variability of soil hydraulic and soil hydrological properties of two Northern German soils. *Geoderma*, *145*, 295–302. https://doi.org/10.1016/j.geoderma.2008.03.017

Chahinian, N., Moussa, R., Andrieux, P., & Voltz, M. (2005). Comparison of infiltration models to simulate flood events at the field scale. *Journal of Hydrology*, *306*, 191–214. https://doi.org/10.1016/j.jhydrol.2004.09.009

Chow, V. (1959). Open Channel Hydraulics [McGraw-Hill Book Company, NY].

Chumchean, S., Sharma, A., & Seed, A. (2003). Radar rainfall error variance and its impact on radar rainfall calibration. *Physics and Chemistry of the Earth, Parts A/B/C*, *28*(1-3), 27–39. https://doi.org/10.1016/S1474-7065(03)00005-6

Copernicus. (n.d.). Land Cover and Land Use Mapping. https://land.copernicus.eu/en/map-viewer

de Doncker, L., Troch, P., Verhoeven, R., Bal, K., Meire, P., & Quintelierk, J. (2009). Determination of the Manning roughness coefficient influenced by vegetation in the river Aa and Biebrza river. *Environmental Fluid Mechchanics*, *9*, 549–567. https://doi.org/10.1007/s10652-009-9149-0

Department of Mineral Resources. (2008). Geological map of Changwat Phetchaburi. https://gisportal.dmr.go.th/portal/apps/MapSeries/index.html?appid=927a0f2c42f44c40ab6cb03109682ebf

ESCAP. (2017). Leave No One behind: Disaster Resilience for Sustainable Development: Asia-Pacific Disaster Report 2017 [Report for Sustainable Development, United Nations Economic and Social Commission for Asia and the Pacific, Bangkok].

Gires, A., Onof, C., Maksimovic, C., Schertzer, D., Tchiguirinskaia, I., & Simoes, N. (2012). Quantifying the impact of small scale unmeasured rainfall variability on urban runoff through multifractal downscaling: A case study. *Journal of Hydrology*, *442–443*, 117–128. https://doi.org/10.1016/j.jhydrol.2012.04.005

Goovaerts, P. (2000). Geostatistical approaches for incorporating elevation into the spatial interpolation of rainfall. *Journal of Hydrology*, *228*, 113–129. https://doi.org/10.1016/S0022-1694(00)00144-X

Guo, B., Zhang, J., Xu, T., Song, Y., Liu, M., & Dai, Z. (2022). Assessment of multiple precipitation interpolation methods and uncertainty analysis of hydrological models in Chaohe River basin, China. *Water SA*, *48*(3), 324–334. https://doi.org/10.17159/wsa/2022.v48.i3.3884

Haberlandt, U. (2007). Geostatistical interpolation of hourly precipitation from rain gauges and radar for a large-scale extreme rainfall event. *Journal of Hydrology*, *332*, 144–157. https://doi.org/10.1016/j.jhydrol.2006.06.028

Hazenberg, P., Leijnse, H., & Uijlenhoet, R. (2011). Radar rainfall estimation of stratiform winter precipitation in the Belgian Ardennes. *Water Resources Research*, *47*(2). https://doi.org/10.1029/2010WR009068

HEC-RAS. (n.d.). HEC-RAS Mapper User's Manual. https://www.hec.usace.army.mil/confluence/rasdocs/rmum/latest

HEC-RAS. (2024). HEC-RAS Hydraulic Reference Manual Version 6.5. https://www.hec.usace.army.mil/confluence/rasdocs/ras1dtechref/latest

Kimuli, J. B., Di, B., Zhang, R., Wu, S., Li, J., & Yin, W. (2021). A multisource trend analysis of floods in Asia-Pacific 1990–2018: Implications for climate change in sustainable development goals. *International Journal of Disaster Risk Reduction*, *59*. https://doi.org/10.1016/j.ijdrr.2021.102237

Liu, Z., Ma, D., Hu, W., & Li, X. (2018). Land use dependent variation of soil water infiltration characteristics and their scale-specific controls. *Soil and Tillage Research*, *178*, 139–149. https://doi.org/10.1016/j.still.2018.01.001

Lloyd, C. (2005). Assessing the effect of integrating elevation data into the estimation of monthly precipitation in Great Britain. *Journal of Hydrology*, *308*, 128–150. https://doi.org/10.1016/j.jhydrol.2004.10.026

Loritz, R., Hrachowitz, M., Neuper, M., & Zehe, E. (2021). The role and value of distributed precipitation data in hydrological models. *Hydrology and Earth System Sciences*, *25*, 147–167. https://doi.org/10.5194/hess-25-147-2021

Marani, M. (2005). Non-power-law-scale properties of rainfall in space and time. *Water Resources Research*, *41*(8). https://doi.org/10.1029/2004WR003822

Mongil-Manso, J., Jiménez-Ballesta, R., Navarro-Hevia, J., & Martín, R. S. (2025). Soil infltration rates in mediterranean mountain areas: relationship with soil properties and diferent land-use. *European Journal of Forest Research*. https://doi.org/10.1007/s10342-025-01757-6

Nicótina, L., Alessi Celegon, E., Rinaldo, A., & Marani, M. (2008). On the impact of rainfall patterns on the hydrologic response. *Water Resources Research*, *44*(12). https://doi.org/10.1029/2007WR006654

Onarun, T., Thepprasit, C., & Sittichok, K. (2023). Development of statistical downscaling methods for the assessment of rainfall characteristics under climate change scenarios. *Journal of Water and Climate Change*, *14*(9). https://doi.org/10.2166/wcc.2023.490

Pellicone, G., Caloiero, T., Modica, G., & Guagliardi, I. (2018). Application of several spatial interpolation techniques to monthlyrainfall data in the Calabria region (southern Italy). *International Journal of Climatology*, *38*(9), 3475–3748. https://doi.org/10.1002/joc.5525

Schwartz, R. C., Evett, S. R., & Unger, P. W. (2003). Soil hydraulic properties of cropland compared with reestablished and native grassland. *Geoderma*, *116*, 47–60. https://doi.org/10.1016/S0016-7061(03)00093-4

Silva, E. J. R. d., Alves, C. N., Campos, P. C. d. O., Oliveira, R. A. A. C. e., Marques, M. E. S., Amorim, J. C. C., & Paz, I. (2022). Comparison of Rain Gauge Network and Weather Radar Data: Case Study in Angra dos Reis, Brazil. *Water*, *14*, 3944. https://doi.org/10.3390/w14233944

Singh, V. P. (1997). Effect of spatial and temporal variability in rainfall and watershed characteristics on stream flow hydrograph. *Hydrological Processes*, *11*(12), 1573–1682. https://doi.org/10.1002/(SICI)1099-1085(19971015)11:12<1649::AID-HYP495>3.0.CO;2-1

SoilGrids. (n.d.). Soil Classification. https://soilgrids.org/

Sreesomjai, P. (2024). Inflow Prediction System for Kaeng Krachan Reservoir Using Radar Rainfall Technologies [Project by the Royal Irrigation Department and Kasetsart University].

Sun, N., Huang, W., Creed, M., & Sun, X. (2025). Impact of Spatial Distribution Methods for Rainfall on Flash Floods Modelling Using a Hydrodynamic Model. *Journal of Flood Risk Management*, *18*(1). https://doi.org/10.1111/jfr3.70010

Terink, W., Leijnse, H., van den Eertwegh, G., & Uijlenhoet, R. (2018). Spatial resolutions in areal rainfall estimation and their impact on hydrological simulations of a lowland catchment. *Journal of Hydrology*, *563*, 319–335. https://doi.org/10.1016/j.jhydrol.2018.05.045

Thiessen, A. H. (1911). Precipitation averages for large areas. *Monthly Weather Review*, *39*(7), 1082–1089. https://doi.org/10.1175/1520-0493(1911)39<1082b:PAFLA>2.0.CO;2

Trenberth, K. E. (2011). Changes in precipitation with climate change. *Climate Research*, *47*, 123–138. https://doi.org/10.3354/cr00953

Uijlenhoet, R., & Berne, A. (2008). Stochastic simulation experiment to assess radar rainfall retrieval uncertainties associated with attenuation and its correction. *Hydrology and Earth System Sciences*, *12*(2), 587–601. https://doi.org/10.5194/hess-12-587-2008

van de Beek, C. Z., Leijnse, H., Stricker, J. N. M., Uijlenhoet, R., & Russchenberg, H. W. J. (2010). Performance of high-resolution X-band radar for rainfall measurement in The Netherlands. *Hydrology and Earth System Sciences*, *14*(2). https://doi.org/10.5194/hess-14-205-2010

Vozinaki, A.-E. K., Morianou, G. G., Alexakis, D. D., & Tsanis, I. K. (2017). Comparing 1D and combined 1D/2D hydraulic simulations usinghigh-resolution topographic data: a case study of the Koiliaris basin, Greece. *Hydrological Sciences Journal*, *62*(4), 642–656. https://doi.org/10.1080/02626667.2016.1255746

Watson, D. (1987). Hydraulic effects of aquatic weeds in U.K. rivers. *Regulated Rivers: Research & Management*, *1*(3), 211–227. https://doi.org/10.1002/rrr.3450010303

A

Geology of the Phetchaburi river basin

In the west of the Phetchaburi river basin, the geology mostly consists of graywacke. The national park is located here and it is a mountainous area. Further to the east, still some graywacke can be found, but colluvial deposits can also be found with alluvial and fluvial deposits around the rivers. In the far east, mostly tidal flat deposits can be found.

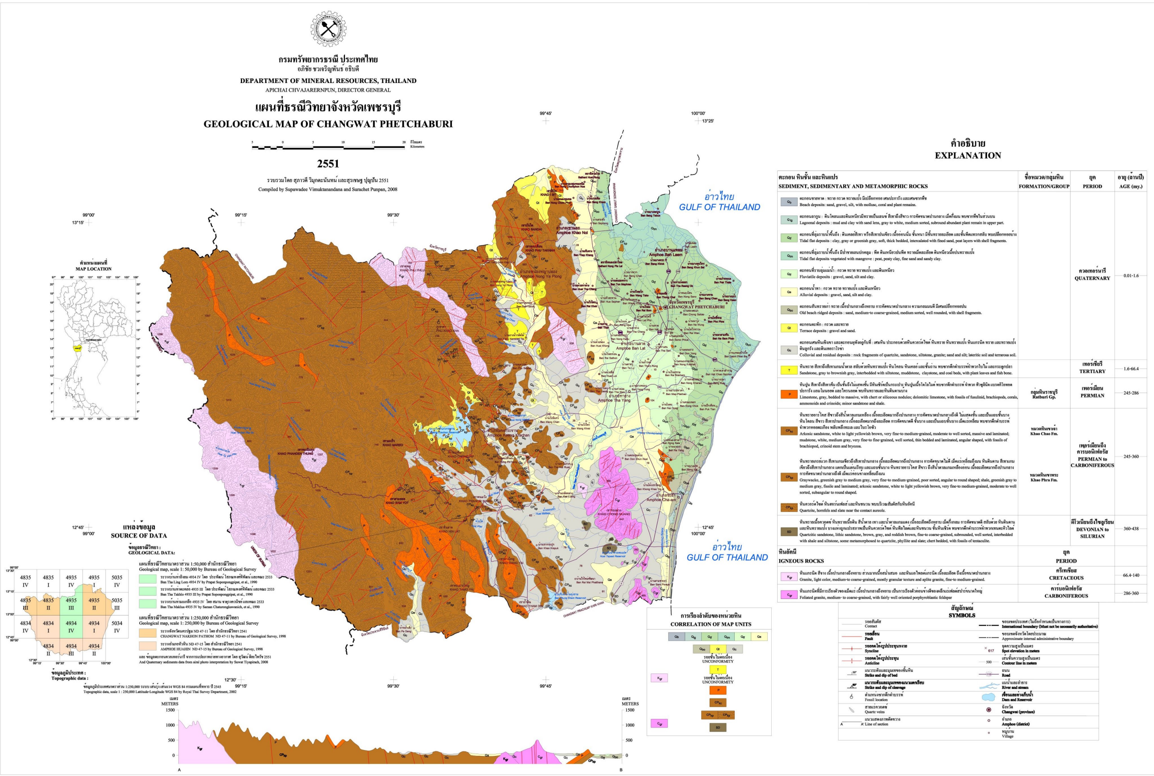

Figure A.1: Geology map of the Phetchaburi province (Department of Mineral Resources, 2008).

B

Daily precipitation data from the rain gauges in the Phetchaburi river basin

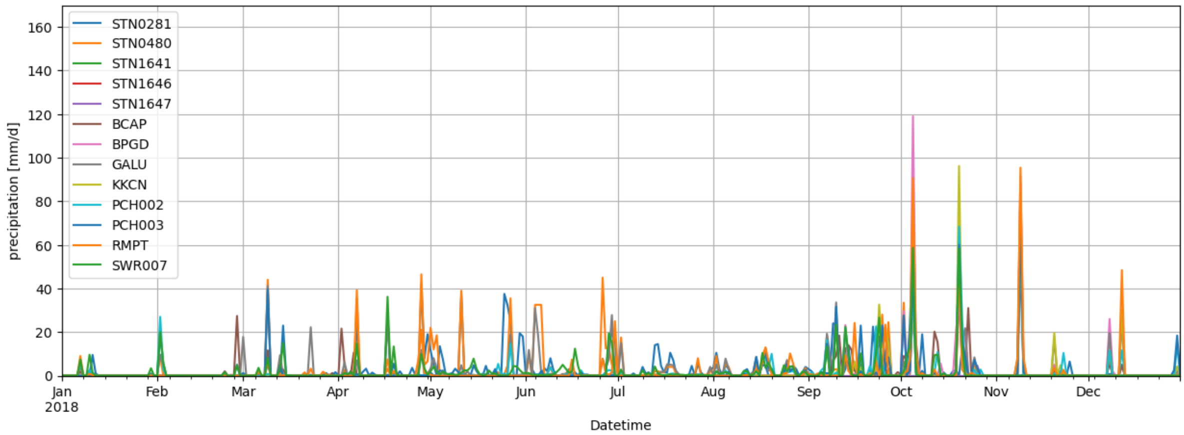

Figure B.1: Daily precipitation data from rain gauges for the year 2018.

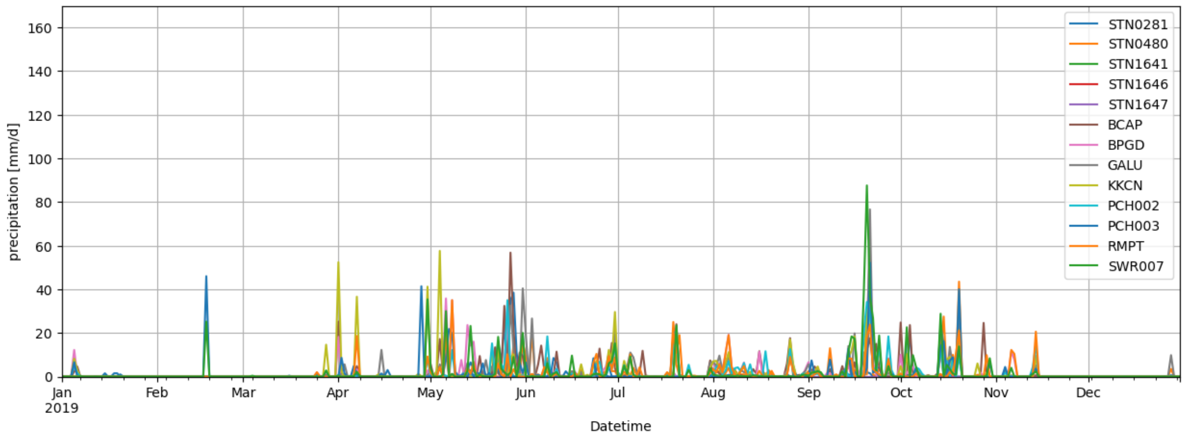

Figure B.2: Daily precipitation data from rain gauges for the year 2019.

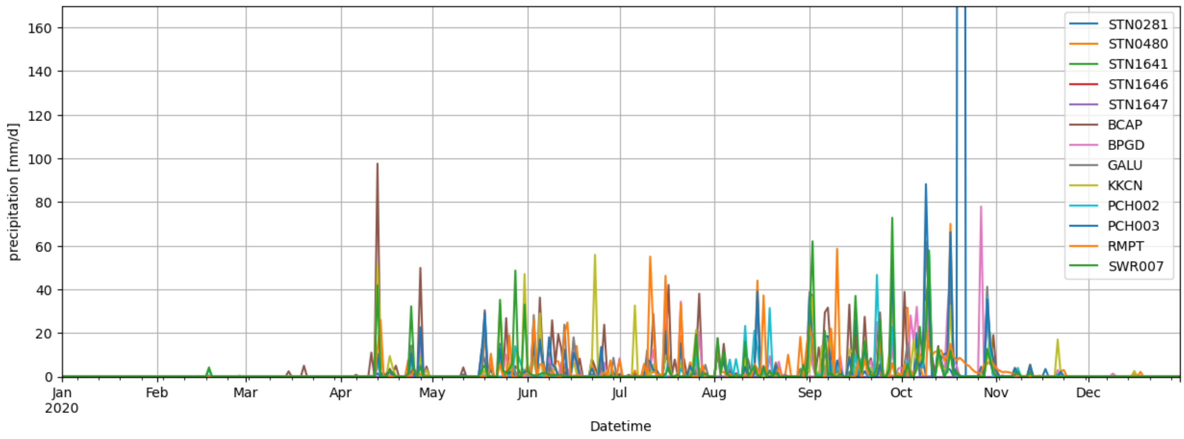

Figure B.3: Daily precipitation data from rain gauges for the year 2020. Data from station STN0281 is cut off because it has a few unrealistic values.

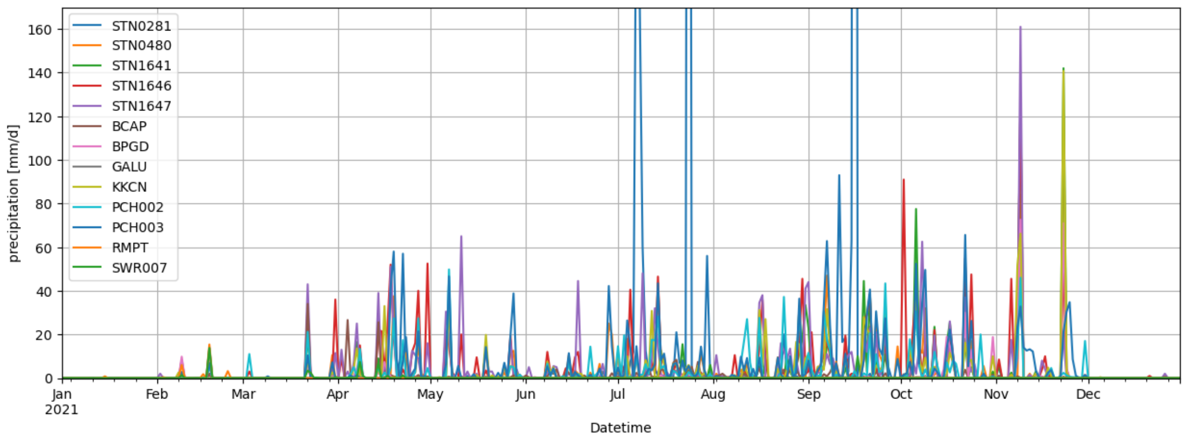

Figure B.4: Daily precipitation data from rain gauges for the year 2021. Data from station STN0281 is cut off because it has a few unrealistic values.

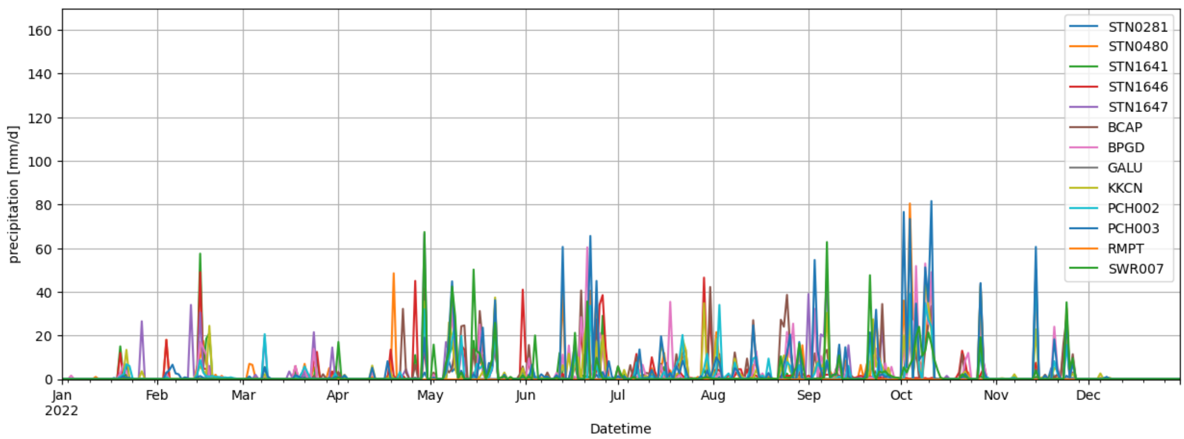

Figure B.5: Daily precipitation data from rain gauges for the year 2022.

C

Locations of the four cross sections of the Phetchaburi river

Four locations on the Phetchaburi river were chosen to show the water levels in Figure 5.7 in Chapter 5. The cross section at location 1 is right upstream of the Phet Diversion Dam. Locations 2, 3 and 4 are locations where the Phetchaburi river is sensitive to floods.

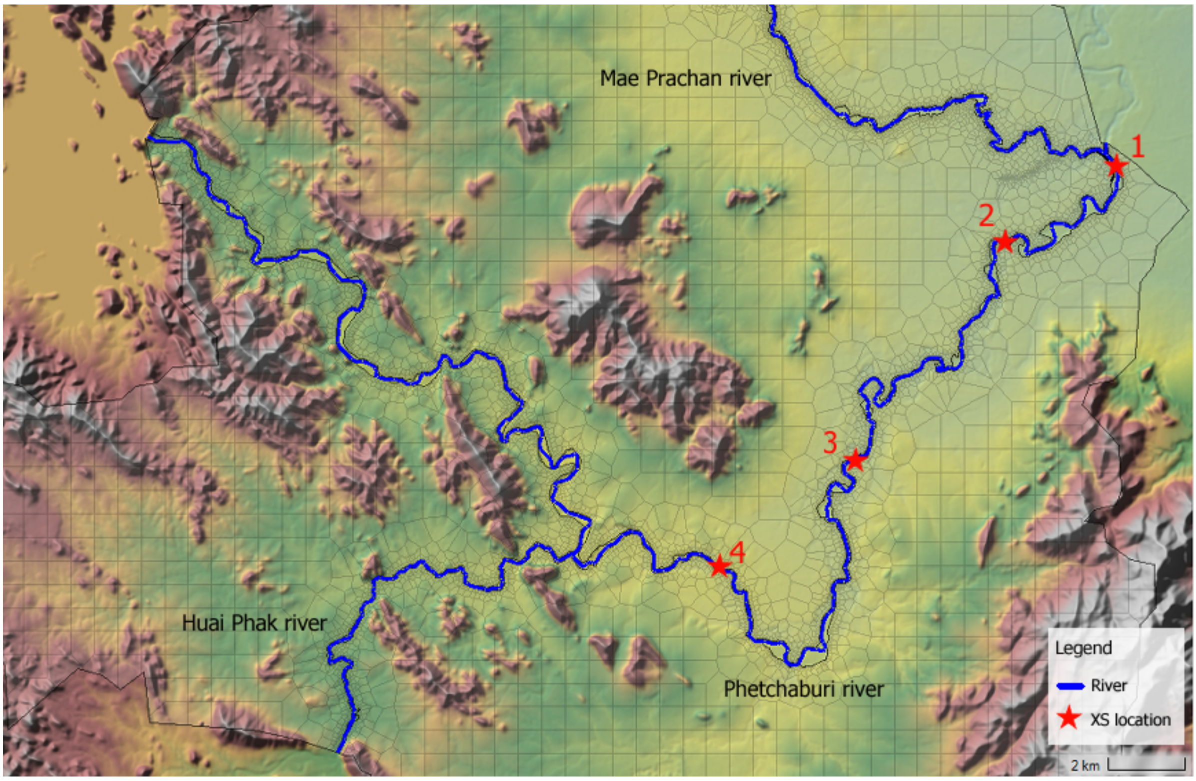

Figure C.1: Locations of the four cross sections of the Phetchaburi river.

D

Modelled water levels at each station

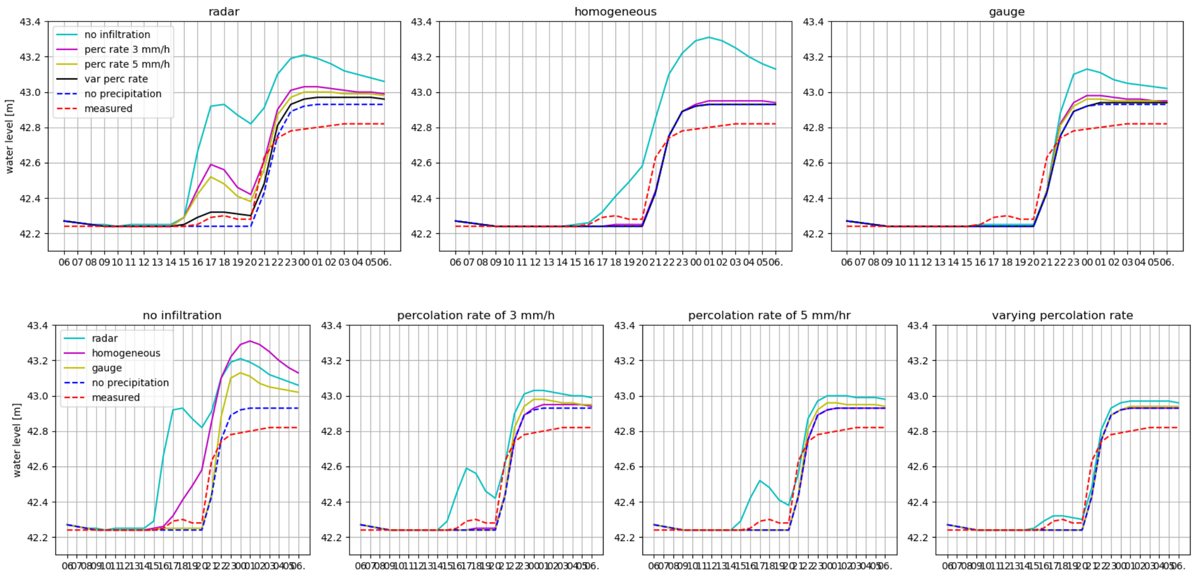

Figure D.1: Water levels for each infiltration and precipitation data type scenario at station B.3A upstream on the Phetchaburi river for event 2.1.

Table D.1: RMSE of the modelled water levels at station B.3A upstream on the Phetchaburi river for event 2.1.

Scenario	**Radar RMSE [m]**	**Homogeneous RMSE [m]**	**Gauge RMSE [m]**
No infiltration	0.330	0.268	0.159
Perc rate 3 mm/hr	0.157	0.086	0.099
Perc rate 5 mm/hr	0.132	0.080	0.092
Var perc rate	0.095	0.080	0.083

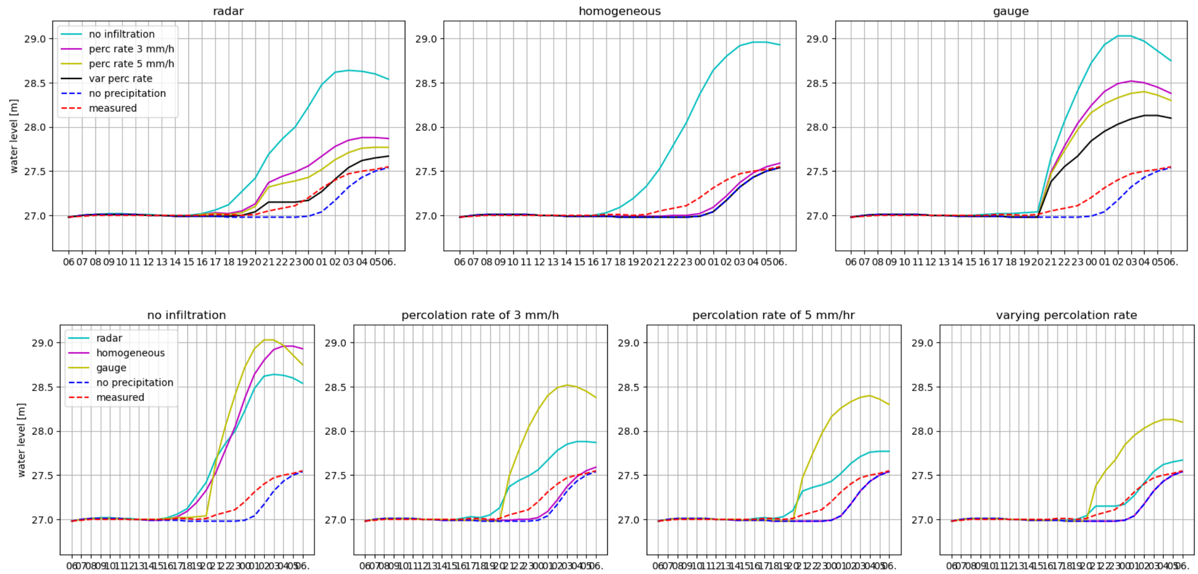

Figure D.2: Water levels for each infiltration and precipitation data type scenario at station B.9 downstream on the Phetchaburi river for event 2.1.

Table D.2: RMSE of the modelled water levels at station B.9 downstream on the Phetchaburi river for event 2.1.

Scenario	**Radar RMSE [m]**	**Homogeneous RMSE [m]**	**Gauge RMSE [m]**
No infiltration	0.657	0.777	0.859
Perc rate 3 mm/hr	0.230	0.078	0.589
Perc rate 5 mm/hr	0.158	0.097	0.527
Var perc rate	0.054	0.097	0.364

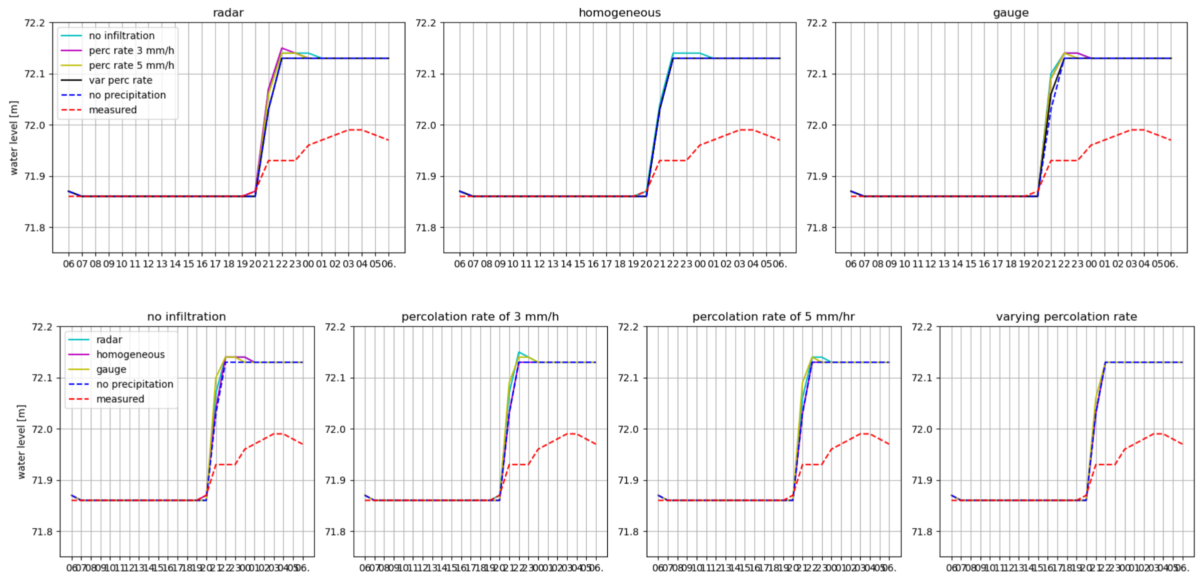

Figure D.3: Water levels for each infiltration and precipitation data type scenario at station B.11 upstream on the Mae Prachan river for event 2.1.

Table D.3: RMSE of the modelled water levels at station B.11 upstream on the Mae Prachan river for event 2.1.

Scenario	Radar RMSE [m]	Homogeneous RMSE [m]	Gauge RMSE [m]
No infiltration	0.105	0.104	0.106
Perc rate 3 mm/hr	0.105	0.101	0.106
Perc rate 5 mm/hr	0.104	0.101	0.105
Var perc rate	0.101	0.101	0.102

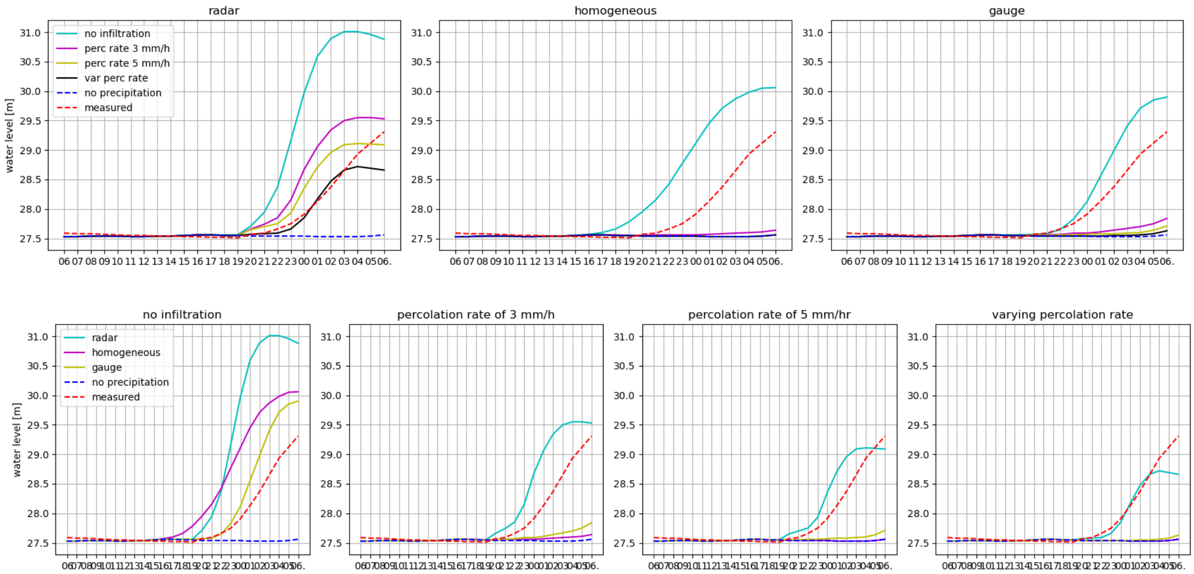

Figure D.4: Water levels for each infiltration and precipitation data type scenario at station B.6A downstream on the Mae Prachan river for event 2.1.

Table D.4: RMSE of the modelled water levels at station B.6A downstream on the Mae Prachan river for event 2.1.

Scenario	Radar RMSE [m]	Homogeneous RMSE [m]	Gauge RMSE [m]
No infiltration	1.184	0.669	0.327
Perc rate 3 mm/hr	0.398	0.603	0.547
Perc rate 5 mm/hr	0.222	0.634	0.592
Var perc rate	0.167	0.634	0.617

Table D.5: RMSE of the modelled water levels at station B.8A on the Huai Phak river for event 2.1.

Scenario	Radar RMSE [m]	Homogeneous RMSE [m]	Gauge RMSE [m]
No infiltration	0.301	0.443	0.261
Perc rate 3 mm/hr	0.123	0.100	0.115
Perc rate 5 mm/hr	0.101	0.118	0.094
Var perc rate	0.091	0.118	0.081

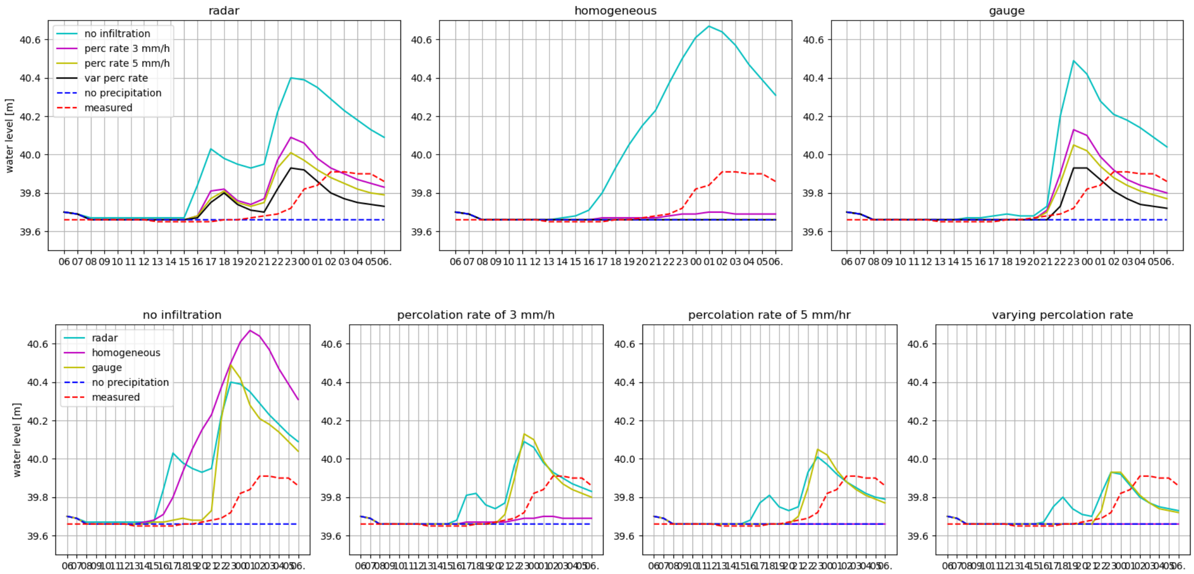

Figure D.5: Water levels for each infiltration and precipitation data type scenario at station B.8A on the Huai Phak river for event 2.1.

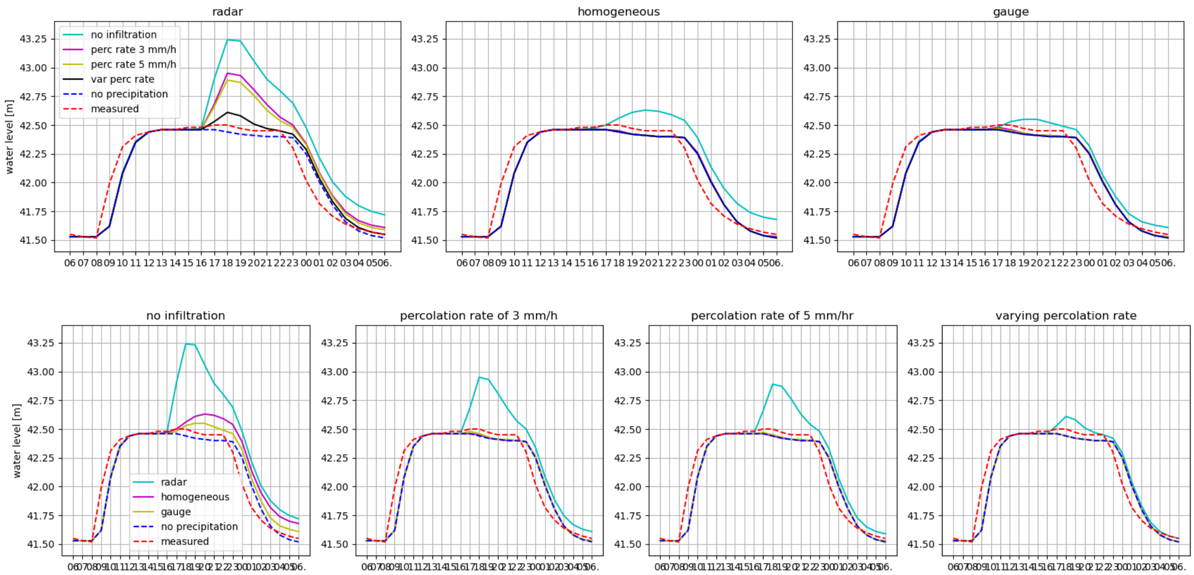

Figure D.6: Water levels for each infiltration and precipitation data type scenario at station B.3A upstream on the Phetchaburi river for event 2.2.

Table D.6: RMSE of the modelled water levels at station B.3A upstream on the Phetchaburi river for event 2.2.

Scenario	Radar RMSE [m]	Homogeneous RMSE [m]	Gauge RMSE [m]
No infiltration	0.343	0.172	0.133
Perc rate 3 mm/hr	0.211	0.114	0.113
Perc rate 5 mm/hr	0.191	0.113	0.114
Var perc rate	0.123	0.113	0.113

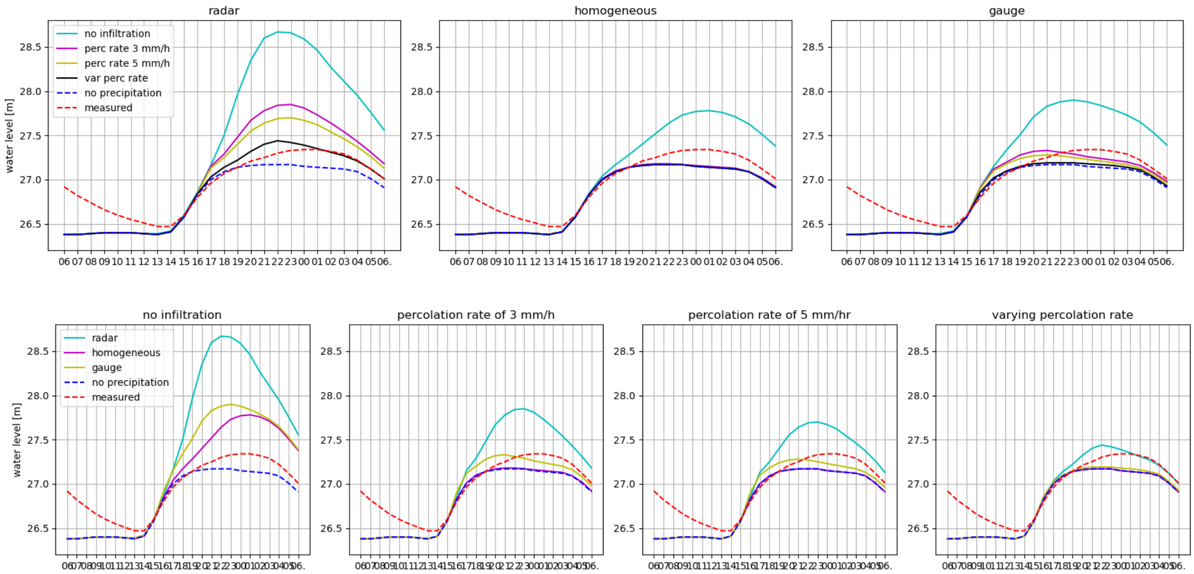

Figure D.7: Water levels for each infiltration and precipitation data type scenario at station B.9 downstream on the Phetchaburi river for event 2.2.

Table D.7: RMSE of the modelled water levels at station B.9 downstream on the Phetchaburi river for event 2.2.

Scenario	**Radar RMSE [m]**	**Homogeneous RMSE [m]**	**Gauge RMSE [m]**
No infiltration	0.798	0.341	0.426
Perc rate 3 mm/hr	0.360	0.151	0.171
Perc rate 5 mm/hr	0.293	0.152	0.163
Var perc rate	0.176	0.152	0.150

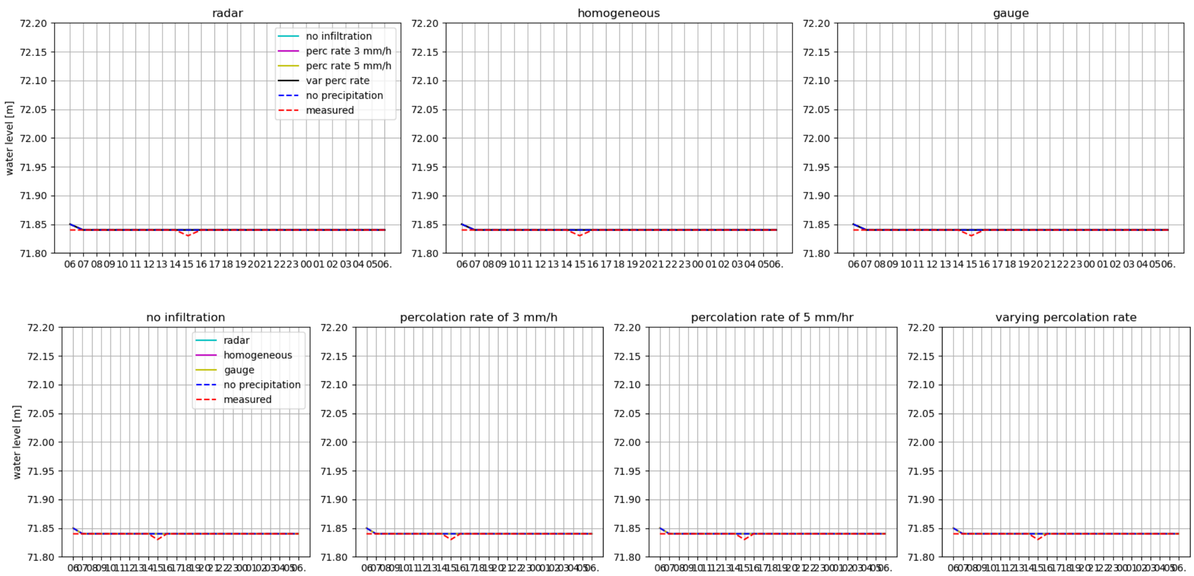

Figure D.8: Water levels for each infiltration and precipitation data type scenario at station B.11 upstream on the Mae Prachan river for event 2.2.

Table D.8: RMSE of the modelled water levels at station B.11 upstream on the Mae Prachan river for event 2.2.

Scenario	Radar RMSE [m]	Homogeneous RMSE [m]	Gauge RMSE [m]
No infiltration	0.003	0.003	0.003
Perc rate 3 mm/hr	0.003	0.003	0.003
Perc rate 5 mm/hr	0.003	0.003	0.003
Var perc rate	0.003	0.003	0.003

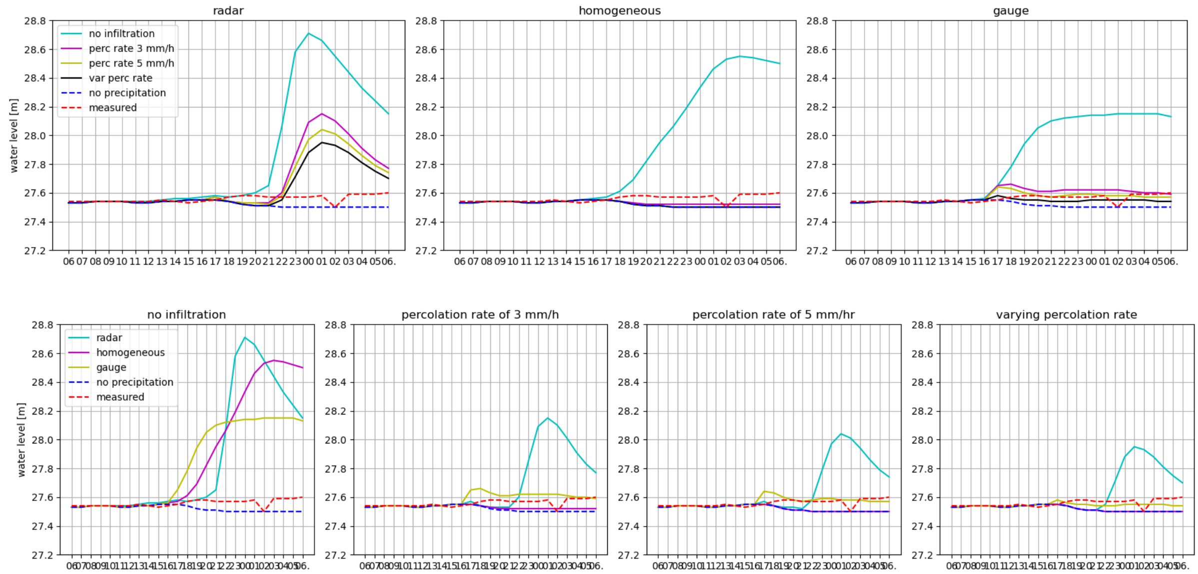

Figure D.9: Water levels for each infiltration and precipitation data type scenario at station B.6A downstream on the Mae Prachan river for event 2.2.

Table D.9: RMSE of the modelled water levels at station B.6A downstream on the Mae Prachan river for event 2.2.

Scenario	Radar RMSE [m]	Homogeneous RMSE [m]	Gauge RMSE [m]
No infiltration	0.523	0.520	0.379
Perc rate 3 mm/hr	0.237	0.042	0.044
Perc rate 5 mm/hr	0.194	0.053	0.030
Var perc rate	0.157	0.053	0.028

Table D.10: RMSE of the modelled water levels at station B.8A on the Huai Phak river for event 2.2.

Scenario	Radar RMSE [m]	Homogeneous RMSE [m]	Gauge RMSE [m]
No infiltration	0.211	0.069	0.106
Perc rate 3 mm/hr	0.170	0.269	0.262
Perc rate 5 mm/hr	0.180	0.275	0.266
Var perc rate	0.208	0.275	0.270

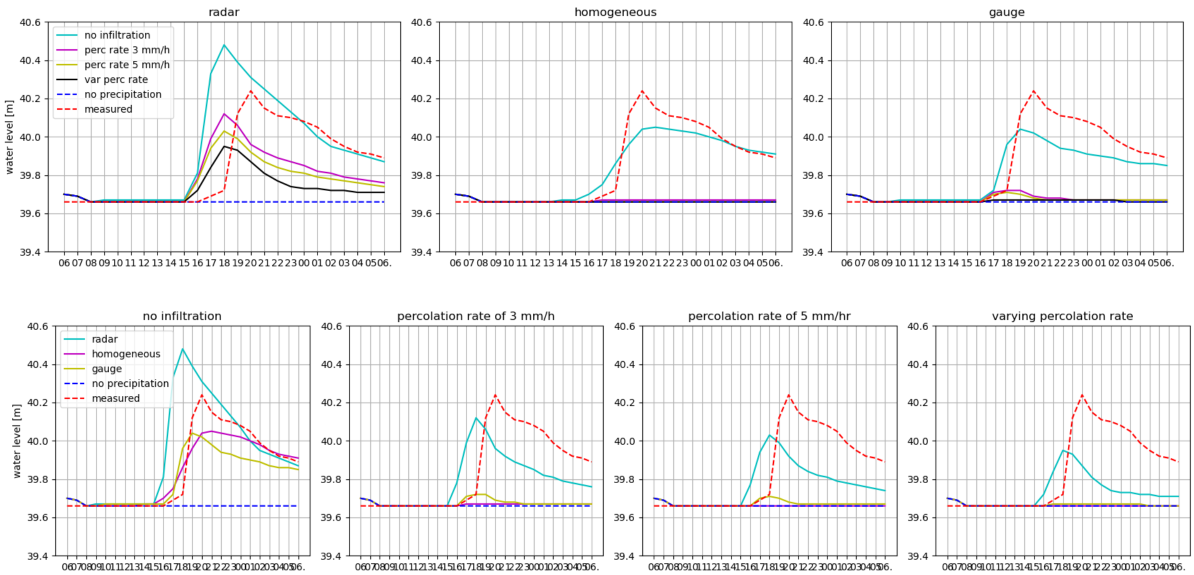

Figure D.10: Water levels for each infiltration and precipitation data type scenario at station B.8A on the Huai Phak river for event 2.2.